

✓
**SYNTHESIS, CHARACTERIZATION AND
CATALYTIC PROPERTIES OF TITANIUM
SILICALITE-1 (TS-1) CATALYST : n-HEXANE
OXIDATION KINETICS AND MODELING
STUDIES**

*A Thesis Submitted
in Partial Fulfilment of the Requirements
for the Degree of
MASTER OF TECHNOLOGY*


by
M. SHYAM SUNDAR

to the
DEPARTMENT OF CHEMICAL ENGINEERING
INDIAN INSTITUTE OF TECHNOLOGY, KANPUR
March, 1994

29/3/94
B3

CERTIFICATE

This is to certify that the present work entitled " SYNTHESIS, CHARACTERIZATION AND CATALYTIC PROPERTIES OF TITANIUM SILICALITE-1 (TS-1) CATALYST : n-HEXANE OXIDATION KINETICS AND MODELING STUDIES " has been carried out by Mr.M. SHYAM SUNDAR under my supervision and has not been submitted elsewhere for a degree.


29/03/94

Dr.S. Bhatia

Professor

Department of Chemical Engineering

Indian Institute of Technology

Kanpur-208 016

March, 1994.

CHE-1994-M-SUN-SYN

21 APR 1994

CENTRAL LIBRARY
1111 E. 10th St.

Doc. No. A. 117708

DEDICATED
TO MY
PARENTS
AND
FRIENDS

ACKNOWLEDGEMENTS

I am vastly indebted to my thesis guide Dr. S. Bhatia without whom this work would not have been possible. I am sure, the way he guided me will help me throughout my life.

I am grateful to Mr. Virdhi who had helped me a lot during my experiments. I am thankful to Dr. M.S. Rao who had given me the column for my analysis work.

Prem, T, Sharma, Venu, Reddy, Kishore, Manda and Sudhakar have given me the taste of true friendship during my stay at IIT Kanpur. They have helped me a lot whenever I was in need. My sincere thanks to them.

I would like to thank Mr. N. Srinivas who had helped me a lot in typing this thesis. I would like to thank everybody who brightened my stay at IIT Kanpur.

Finally, to my parents and brothers goes my eternal gratitude for their love and support.

M. Shyam Sundar

CONTENTS

List of Figures

List of Tables

Nomenclature

Abstract

| | | |
|--------|-------------------------|----|
| 1. | Introduction | 1 |
| 2. | Experimental Section | 10 |
| 2.1 | Catalyst Preparation | 11 |
| 2.2 | Experimental Set-up | 12 |
| 2.3 | Experimental Procedure | 14 |
| 2.3.1. | Kinetic Study | 14 |
| 2.3.2. | Product Analysis | 15 |
| 2.3.3 | Calibration | 15 |
| 3. | Kinetic Modelling | 18 |
| 3.1 | Reaction Mechanism | 18 |
| 3.2 | Reaction Modelling | 19 |
| 3.2.1. | Homogeneous Modelling | 19 |
| 3.2.2 | Heterogeneous Modelling | 23 |

| | | |
|--------|---|----|
| 3.3 | Optimization Studies | 27 |
| 3.3.1. | Response Surface Methodology | 28 |
| 3.3.2. | First Move on the Response Surface | 29 |
| 3.3.3. | Selection of Experimental Design | 30 |
| 3.3.4. | Model Fitting | 30 |
| 3.3.5 | Calculation of the path of Steepest Ascent and Conduct of Experiments Along this Path | 31 |
| 4. | Results and Discussion | 32 |
| 4.1 | Reproducibility of Kinetic Data | 33 |
| 4.2 | Effect of Important Reaction Variables | 33 |
| 4.2.1. | Effect of Reaction Temperature | 33 |
| 4.2.2. | Effect of Reaction Time on Conversion of <i>n</i> -Hexane. | 36 |
| 4.2.3. | Effect of % Catalyst Loading on Oxidation of <i>n</i> -Hexane. | 39 |
| 4.2.4. | Effect of Hydrogen Peroxide/ <i>n</i> -hexane Mole ratio on Oxidation of <i>n</i> -Hexane. | 39 |
| 4.2.5. | Effect of Titanium Content in <i>TS</i> – 1 on Oxidation of <i>n</i> -Hexane and Comparision with TiZSM5-5 and ZSM-5 Catalysts. | 39 |
| 4.3. | Optimum values of Reaction Variables | 43 |
| 4.3.1. | Model Fitting | 43 |
| 4.3.2 | Calculation of the Path of Steepest Ascent and Conduct of Experiments Along this Path. | 46 |

| | Page No. |
|--|----------|
| 4.4 Characterization Studies | 52 |
| 4.4.1 X-Ray Diffraction of $TS - 1$ Catalyst | 52 |
| 4.4.2 Infra Red Spectroscopy | 58 |
| 4.4.3 Scanning Electron Microscopy | 58 |
| 4.5 Kinetic Modelling | 62 |
| 4.5.1 Homogeneous Model | 62 |
| 4.5.2 Heterogeneous Model | 66 |
| 5. Conclusions and Recommendations | 83 |
| 5.1 Conclusions | 83 |
| 5.2 Recommendations | 84 |
| References | 85 |
| Appendix A | |

List of Figures

| | | |
|----------|--|----|
| Fig 2.1 | Schematic Diagram of the Experimental Setup | 23 |
| Fig 2.2 | A Typical Chromatogram | 24 |
| Fig 4.1 | Reproducibility of Experimental Data (<i>TS</i> – 1 Catalyst, Time = 8 hours, % Catalyst Loading = 1.5, H_2O_2/n -hexane Mole Ratio = 0.2) | 34 |
| Fig 4.2 | Effect of Temperature on <i>n</i> -Hexane Conversion (<i>TS</i> – 1 Catalyst, Time = 8 hours, % Catalyst Loading = 1.5, H_2O_2/n -hexane Mole Ratio = 0.2) | 35 |
| Fig 4.3 | Effect of Reaction Time on Conversion of <i>n</i> -Hexane (<i>TS</i> – 1 Catalyst, Temperature = 353-393 K, % Catalyst Loading = 1.5, H_2O_2/n - Hexane Mole Ratio = 0.2) | 37 |
| Fig 4.4 | Effect of Reaction Time on Concentration of <i>n</i> -Hexane Temperature = 353-393 K, % Catalyst Loading = 1.5, H_2O_2/n - Hexane Mole Ratio = 0.2) | 38 |
| Fig 4.5 | Effect of % Catalyst Loading on Conversion of <i>n</i> -Hexane, Yield of Hexanol + Hexanone, Selectivities of Hexanol and Hexanone (Time = 8.48 hours, Temperature = 377 K, H_2O_2/n -hexane mole ratio = 1.4) | 40 |
| Fig 4.6 | Effect of H_2O_2/n -Hexane Mole Ratio on Conversion of <i>n</i> -Hexane, Yield of Hexanol + Hexanone, Selectivities of Hexanol and Hexanone (Time = 8.48 hours, Temperature = 377K % Catalyst Loading = 2.33) | 41 |
| Fig 4.7 | Effect of <i>Ti</i> Content in <i>TS</i> – 1 Catalyst on Conversion of <i>n</i> -Hexane, Yield of Hexanol + Hexanone, Selectivities of Hexanol and Hexanone (Time = 8 hours, Temperature = 377K % Catalyst Loading = 2.33, H_2O_2/n -Hexane Mole Ratio = 1.4) | 42 |
| Fig 4.8a | X-Ray Diffraction Pattern of ZSM-5 Catalyst | 55 |
| Fig 4.8b | X-Ray Diffraction Pattern of Fresh <i>TS</i> – 1 Catalyst | 56 |
| Fig 4.8c | X-Ray Diffraction Pattern of Regenerated <i>TS</i> – 1 Catalyst | 57 |
| Fig 4.9 | Infra Red Spectra of <i>TS</i> – 1 Catalysts | 59 |

| | | |
|-----------|--|----|
| Fig 4.10a | SEM Micrograph of $TS - 1$ Catalyst Before Calcination | 60 |
| Fig 4.10b | SEM Micrograph of $TS - 1$ Catalyst After Calcination ($Ti/(Ti + Si) = 0.029$) | 60 |
| Fig 4.10c | SEM Micrograph of $TS - 1$ with $Ti/(Ti + Si) = 0.035$ | 61 |
| Fig 4.10d | SEM Micrograph of TiZSM-5 | 61 |
| Fig 4.11 | Arrhenius Plot of Reaction Rate Constants (Homogeneous Model). Curves (1) k_1 (2) k_2 | 65 |
| Fig 4.12 | Arrhenius Plot of Reaction Rate Constants (Heterogeneous Model). Curves (1) k_{sr1} (2) k_{sr2} | 69 |
| Fig 4.13 | Arrhenius Plot of Reaction Rate Constants (Heterogeneous Model). Curves (1) K_{A1} (2) K_{D1} (3) K_{D2} | 70 |
| Fig 4.14 | % Yield of Hexanol + Hexanone versus Time (Temperature = 353-393 K, % Catalyst Loading = 1.5, H_2O_2/n -Hexane Mole Ratio = 0.2) | 72 |
| Fig 4.15 | % Selectivity of Hexanol versus Time (Temperature = 353-393 K, % Catalyst Loading = 1.5, H_2O_2/n -Hexane Mole Ratio = 0.2) | 73 |
| Fig 4.16 | % Selectivity of Hexanone versus Time (Temperature = 353-393 K, % Catalyst Loading = 1.5, H_2O_2/n -Hexane Mole Ratio = 0.2) | 74 |
| Fig 4.17 | Rate versus Time (Temperature = 353-393 K, % Catalyst Loading = 1.5, H_2O_2/n -Hexane Mole Ratio = 0.2) | 75 |
| Fig 4.18 | Comparison of Experimental versus Calculated Values of Rate of n -Hexane Over $TS - 1$ Catalyst | 79 |
| Fig 4.19 | Comparison of Experimental versus Calculated Values of % Conversion of n -Hexane Over $TS - 1$ Catalyst | 80 |
| Fig 4.20 | Comparison of Experimental versus Calculated Values of % Yield of Hexanol + Hexanone Over $TS - 1$ Catalyst | 81 |
| Fig 4.21 | Comparison of Experimental versus Calculated Values of % Selectivity of Hexanol Over $TS - 1$ Catalyst | 82 |

List of Tables

| | | |
|------------|--|----|
| Table 4.1 | Reaction Variables and their Range | 32 |
| Table 4.2 | <i>n</i> -Hexane Conversion (%) Data Over <i>TS</i> - 1 Catalyst (Reproducibility Data) | 33 |
| Table 4.3 | First Order Response Surface Strategy : Levels of Factors | 44 |
| Table 4.4 | The 2 ^d First Order Design Matrix and Values of Responses | 45 |
| Table 4.5 | First Order Response Surface Strategy : Test for the Adequacy of the Model for % Conversion of <i>n</i> -Hexane | 47 |
| Table 4.6 | First Order Response Surface Strategy : Test for the Adequacy of the Model for % Yield of Hexanol + Hexanone | 48 |
| Table 4.7 | First Order Response Surface Strategy : Test for the Adequacy of the Model for % Selectivity of Hexanol | 49 |
| Table 4.8 | First Order Response Surface Strategy : Calculations for the Path of Steepest Ascent | 51 |
| Table 4.9 | First Order Response Surface Strategy : Results of Experiments Along the Path of Steepest Ascent | 53 |
| Table 4.10 | Optimum Values of Factor Levels for the Maximum % Yield of Hexanol + Hexanone | 54 |
| Table 4.11 | Typical Experimental Kinetic Data on <i>TS</i> - 1 catalyst | 63 |

| | | |
|------------|--|----|
| Table 4.12 | Effect of Reaction Temperature on Rate Constants (Homogeneous Model) | 64 |
| Table 4.13 | Effect of Reaction Temperature on Reaction Parameters over $T'S - 1$ Catalyst (Heterogeneous Model) | 68 |
| Table 4.14 | Values of Activation Energy, Pre-exponential Factors, Heats of Adsorption and Desorption (Heterogeneous Model) | 71 |
| Table 4.15 | Comparison of Experimental and Calculated Values of % Conversion, % Yield, % Selectivities of Hexanol and Hexanone (Heterogeneous Model) | 77 |
| Table 4.16 | Comparison of % Conversion, % Yield and % Selectivities with Reported Values | 78 |

NOMENCLATURE

| | |
|-----------------------|--|
| A | <i>n</i> -Hexane |
| B | Hydrogen peroxide |
| C | Hexanol |
| D | Hexanone |
| C_A, C_B, C_C, C_D | Concentrations of <i>n</i> -hexane, hydrogen-peroxide , hexanol and hexanone |
| C_{A0} | Initial concentration of <i>n</i> -hexane |
| X_A | Conversion of <i>n</i> -hexane |
| Y_Y | Yield of hexanol + hexanone |
| S_1 | Selectivity of hexanol |
| S_2 | Selectivity of hexanone |
| r_A | Rate of disappearance of A |
| r_B | Rate of disappearance of B |
| r_C | Rate of formation of C |
| r_D | Rate of formation of D |
| k_1, k_2 | Homogeneous rate constants |
| k_{10}, k_{20} | Pre-exponential factors |
| k_{sr1}, k_{sr2} | Heterogeneous surface reaction constants |
| K_A, K_{A1}, K_{A2} | Adsorption rate constants |
| K_{D1}, K_{D2} | Desorption rate constants |

| | |
|---|--|
| k_{sr1o}, k_{sr1o} | Arrhenius pre-exponential factors |
| t | time |
| x_1, x_2, x_3, x_4 | Reaction variables like temperature, time, % catalyst loading, H_2O_2 / n -hexane mole ratio |
| x_i | Coded value of i-th factor |
| \bar{x}_i | Natural value of i-th factor |
| \bar{x}_{io} | Natural value of base level of i-th factor |
| v_i | Variation interval of the i-th factor |
| $\hat{b}_0, \hat{b}_1, \hat{b}_2, \hat{b}_3, \hat{b}_4$ | Best fitted values of coefficients |
| \hat{Y} | Predicted response |
| $\hat{\underline{b}}$ | Vector of coefficients |
| \underline{X} | Design matrix |
| \underline{X}^T | Transpose of design matrix |
| \underline{Y} | Vector of responses |
| ϕ | Function describing response surface |
| $\nabla\phi$ | Gradient of response function |
| u_k | Unit vector in the direction of co-ordinate axes |

ABSTRACT

Titanium silicalites are generally used for oxidation reactions using hydrogen peroxide at low temperatures. Titanium Silicalite - 1 ($TS - 1$) was synthesized and characterized using various techniques such as X -ray diffraction (XRD), Scanning electron microscopy (SEM) and Infra-red spectroscopy (IR) etc. Kinetics of n -hexane oxidation with hydrogen peroxide over $TS - 1$ catalyst were studied. The reaction was carried out in a high pressure batch reactor in the temperature range of 353 – 393 K using acetone as solvent. The effect of important variables such as reaction temperature (353 – 393 K), reaction time (3-12 hrs), catalyst loading (1.5% – 3.0%), hydrogen peroxide / n -hexane mole ratio (0.2-1.0) and $Ti/(Ti + Si)$ mole ratio (0.025-0.035) were studied. Conversion, yield and selectivities were calculated and Response surface methodology (RSM) was employed to get the optimum values of the important reaction variables. $TS - 1$ catalysts with different titanium contents were compared with titanium coated ZSM-5 catalyst prepared by chemical vapor deposition technique.

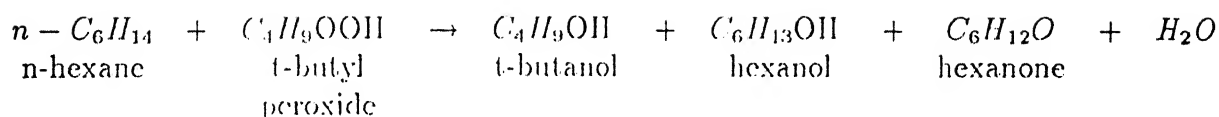
Kinetic data obtained for $TS - 1$ catalyst were analyzed with models based on homogeneous rates and Langmuir-Hinshelwood-Hougen-Watson (LHHW) approach of heterogeneous catalysis. The reaction parameters were evaluated from both the models. The activation energy was found to be 90 KJ/mol from homogeneous model and 140 KJ/mol from heterogeneous model. Conversion, yield and selectivities calculated from the proposed kinetic models were in good agreement with the experimental values confirming validity of the models.

CHAPTER 1

INTRODUCTION

The oxidation of aromatics and alkanes is one of the most important reactions in chemical industry. Extensive research has been done in the oxidation of alkanes to alcohols and ketones. Vanadyl phosphates are selective catalysts for conversion of butane with molecular oxygen into maleic anhydride (Centi et al., 1987). Catalytic conversion of cyclohexane into cyclohexanol and cyclohexanone using a cobalt catalyst is an established industrial process, (Lyons.J.E, 1984). Oxidation of alkanes to alcohols and ketones has been reported (Shilov,A.E, 1984) using $Pd - Fe$ zeolite in an O_2/H_2 atmosphere. The yields proved to be better on zeolite catalysts when compared to the conventional catalysts. Further, all the reactions were carried out in vapor phase. Vapor phase oxidation of n -hexane in the presence of excess air on Cobalt oxide (Co_3O_4) catalysts. Selectivity was found to be very poor and carbondioxide was the major product instead of alcohols and ketones.

Hexanol and Hexanone are important intermediates in many chemical reactions. They are used as antiseptics and for hypnosis. These two were produced by oxidation of n -hexane over solid catalysts. Until now one of the least studied catalyzed reactions is the oxyfunctionalisation of n -hexane in liquid phase. But, the great abundance of n -hexane makes it one of the greatest resources for the energy and chemical industry. n -Hexane was oxidised by a peroxidic source, such as t -butyl hydroperoxide, to the corresponding hexanol and hexanones with maintenance of carbon chain structure, according to the following general scheme:



The catalyst used in the above reaction was iron-phthalocyanines (FePc) in the supercages of zeolite *Y* and in the channels of VPI-5 molecular sieve. The conditions used were ambient temperature and atmospheric pressure. In this reaction, the yield of hexanol + hexanone on FePcY and FePcVPI-5 catalysts was 75% and less than 10% respectively. More over the major side reaction was the decomposition of the organic peroxide to molecular oxygen and tert-butanol.

Owing to the low yields of oxidation products on these catalysts, it was believed that introducing functional groups into the alkanes by oxidation tended to result in severe and thus unselective conditions.

The physicochemical and catalytic behaviour of zeolites can be modified by changing their framework configuration. Isomorphous substitution of metal in the zeolite framework generally resulted in interesting class of metallosilicates which have unique catalytic properties for number of oxidation reactions (Huhrychets et al.,1992). The discovery of the titanium containing MFI type zeolite TS-1 by Enichem workers, led to a remarkable progress in the field of oxidations with hydrogen peroxide. Titanium silicalite-1 was reported to be good oxidation catalyst for n-hexane, direct hydroxylation of benzene derivatives with hydrogen peroxide and synthesis of aldehydes and ketones from primary and secondary alcohols. Basically, it is a titanium containing derivative of Silicalite-1 which in selective way catalyses the oxidation of organic substrates with dilute hydrogen peroxide as oxidant (Notari,B. et al., 1987; Romano,U. et al.,1990). Titanium silicalite has been found to catalyse selective oxidation of organic compounds including *n*-alkanes (Tatsumi,T. et al., 1990; Huybrechts,D.R.C. et al., 1990; Clerici,M.G. et al., 1991)which are normally resistant to oxidation by hydrogen peroxide. The advent of crystalline titanium silicalites with zeolitic

properties has enlarged the domain of zeolite catalysts in oxidation reactions (Reddy, J.S. et al., 1990; Thangaraj, A. et al., 1990). The oxidation processes are advantageous over $TS - 1$ from an environmental point of view, as the side product is water.

A large number of articles have been written about the preparation of silicalites and Al-silicalite (Kuei-Jung Chao et al., 1981) but the incorporation of titanium into the structure asks for a completely different approach. Because titanium ions are not stable at the high pH values normally used in zeolite synthesis, they will form a very stable TiO_2 phase which does not dissolve to $Ti(OH)_4$ species, as silicon, aluminium and gallium would do. Therefore, a completely different synthesis route was used to prevent the formation of this stable TiO_2 phase. To understand the problems of this difficult synthesis, influence of different synthesis parameters on the preparation of $TS - 1$ were investigated by van der Pol et al (1992). The substitution of Al with Ti in the MFI structure ($TS - 1$) was first claimed by Taramasso et al (1988). At first, $TS - 1$ samples had to be prepared according to the methods as described by Enichem. The synthesis of crystalline $TS - 1$ from the alkoxide of Si and Ti in the presence of TPAOH involves the initial hydrolysis of the alkoxides. If there are differences in the relative rates of hydrolysis of the two alkoxides, then the precipitation of the solid TiO_2 or SiO_2 can occur.

Preliminary tests were carried out to examine the hydrolysis behaviour of Si and Ti alkoxides by Thangaraj et al. (1992). Table 1.1 presents their results obtained with various experiments carried with the synthesis of $TS - 1$. It is clear from the table that sequence of addition of reactants plays an important role in the synthesis of Titanium Silicalite.

Table 1.1 Results obtained with the sequence of addition of reactants in the synthesis of Titanium Silicalite

Table 1.1

| Reactants | Observations |
|-----------------------------------|-----------------------|
| 1. A + B | Clear solution |
| 2. C + B | Immediate precipitate |
| 3. C + B (in isopropanol) | Immediate precipitate |
| 4. A + D | Clear solution |
| 5. A + D (in isopropanol) | Clear solution |
| 6. A + D + B | Turbid solution |
| 7. A + D + B (in isopropanol) | Clear solution |
| 8. A + B + E (in iso propanol) | Turbid solution |
| 9. A + C + B | Turbid solution |
| 10. A + C + B (in isopropanol) | Turbid solution |

$R = CH_3, C_2H_5, C_3H_7, C_4H_9$

$A = \text{Tetraethyl orthosilicate}(Si(OEt)_4)$

$B = \text{Tetrapropyl ammonium hydroxide}(TPAOH)$

$C = Ti(OR)_4$

$D = \text{Titanium butoxide}(Ti(OBu)_4)$

$E = \text{Titanium isopropoxide}(Ti(Oisopr)_4)$

The following conclusions were reached from the results of Table 1.1:

- In the presence of TPAOH, SiO_2 is not precipitated from $Si(OC_2H_5)_4$. Monomeric SiO_4^{4-} species stabilized by TPA^+ ions were apparently formed.
- Ti-alkoxides hydrolyze to Ti-hydroxides (which transform to oxide on calcination) in

presence of TPAOH.

- The addition of $Ti(OBu)_4$ to monomeric $Si(OH)_4$ species (stabilized by TPA^+ ions) does not lead to Ti -hydroxide formation. The Ti^{4+} ions are probably stabilized by forming titanium silicate species.
- The addition of $Ti(Oisopro)_4$ (instead of the butoxide) to monomeric $Si(OH)_4$ species causes precipitation of Ti presumably due to the more rapid hydrolysis of the isopropoxide compared to the butoxide.

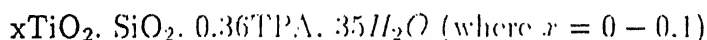
Further, Thangaraj et al. (1992) suggested the modifications in the synthesis of $TS-1$ as follows :

- $Ti(OBu)_4$ was used as the source of titanium instead of the conventional $Ti(OC_2H_5)_4$.
- The $Ti(OBu)_4$ should be dissolved in dry isopropanol to avoid the instantaneous hydrolysis of $Ti(OBu)_4$ to the hydroxide, which results in poor incorporation of Ti .
- The sequence of addition of reactants is modified as shown in the preparation of the catalyst.

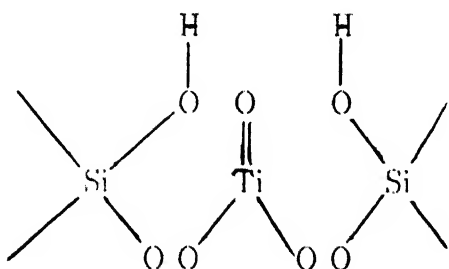
Since the nature of the organic templating agent influences the chemistry of the gel, formed during the synthesis of $TS-1$, it is a critical parameter for the substituted zeolites containing metals other than aluminium. Indeed, one of the conditions for the substitution to occur is the absence of the oxide precipitation during crystallisation. The irreversible formation of TiO_2 oxide particles leads to the reduction in activity by consuming hydrogen peroxide. It is the reason why synthesis of $TS-1$ necessitates a gel mixture capable of directing the MFI structure and preventing the formation of TiO_2 . The use of Na^+ and K^+ ions is, therefore, very unsuitable. That can be achieved using alkali free tetrapropyl

ammonium hydroxide (TPAOH) solutions that supply both the templating agent and the OH^- ions necessary for crystallisation. Because of these restrictive conditions, tetrapropyl ammonium hydroxide is, until now, the single organic molecule that directs the synthesis of *TS* - 1.

Behrens et al. (1991) concluded that Ti^{4+} ions are present mostly in octahedral coordination. They have also suggested that, as a result of the octahedral coordination of these ions, their incorporation in the tetrahedral lattice has to be limited. The highest titanium content reported in literature is 2.5 *Ti* ions/unit cell (*Si/Ti* mole ratio = 39) by Taramasso et al (1988). The size of the crystals was as low as $0.1\mu\text{m}$. The composition of the gel mixture in the formation of *TS* - 1 is as follows:

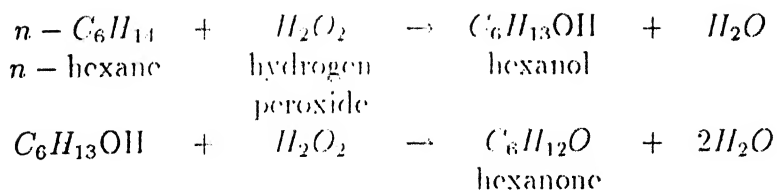


with the following structure:

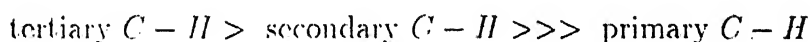


Titanium Silicalite (*TS* - 1) synthesised was characterized by XRD, IR spectroscopy, BET and Scanning electron microscopy.

TS - 1 catalyst was found to be an active catalyst for oxidation of *n*-hexane giving high yield of hexanol + hexanone using hydrogen peroxide as oxidant. The reaction is represented as a series reaction as follows :



The selectivity of hexanol and hexanone was imposed by the shape selective properties of *TS* - 1. Furthermore, it was seen that for branched alkanes, tertiary *C* - *H* bonds were selectively oxidized over secondary ones. The *n*-hexane oxidation on *TS* - 1 thus follows the normal reactivity order:



Furthermore the hexanol + hexanone yield decreased with increasing substrate dimensions. This offered strong evidence for an intracrystalline reaction. Indeed, because of geometrical constraints imposed by pore geometry of *TS* - 1 on the catalyzed reactions, the oxidation rates of organic substrates was proved to decrease as their dimensions increase, and therefore the main side reaction, i.e., thermal and catalytic decomposition of H_2O_2 to O_2 becomes more competitive.

Parton et al. (1990) showed the dependence of *TS* - 1 catalyzed *n*-hexane oxidation on the amount of solvent in the reaction mixture. They showed that *n*-hexane conversion exhibits an optimum against the acetone (solvent) concentration. In absence or at very low concentrations of acetone, the solubility of the organic substrate in the aqueous H_2O_2 phase was low, and therefore the driving force for diffusion of the substrate to this phase was very low. As a result the reaction rate may become diffusion limited. When the amount of acetone was increased, both *n*-hexane solubility and thus the driving force for diffusion increase, which resulted in an increased reaction rate. When the acetone concentration was still further increased however, both H_2O_2 and *n*-hexane became very diluted in the reaction solution, thus causing a decrease in reaction rate. The compromise between high *n*-

hexane solubilities and diffusion rates, and low dilutions explains the optimum of acetone concentration. The transition of a diffusionally to a chemically controlled system with increasing solvent concentration, was confirmed by the results of the above workers, for *n*-hexane oxidation as a function of catalyst concentration both in the presence and absence of acetone. They proved that, in the presence of acetone the *n*-hexane conversion increased in a proportional way with the catalyst concentration. In the absence of a polar solvent deviations of this linearity was observed at low conversions, indicating that the reaction was no longer chemically controlled. They showed that as concentration of acetone increased, ketone/alcohols ratio decreased. The reasoning given by them was that at low acetone concentrations, the *n*-hexane solution and thus the substrate concentration was low, and therefore a hexanol molecule which has been formed on catalyst will be easily converted to hexanone. At higher acetone concentrations and higher *n*-hexane solubilities however, competition between *n*-hexane and hexanol for oxidation will become significant and only a fraction of the hexanol mixture will be further oxidized.

The objectives of the present study are :

- Catalytic activity and selectivity study of *TS* - 1 catalyst for *n*-hexane oxidation using hydrogen peroxide.
- Kinetics study of oxidation reaction.
- Effect of reaction variables such as reaction temperature, reaction time, % catalyst loading, hydrogen peroxide content and titanium content in the catalyst over the conversion, yield and selectivities.
- Use of response surface methodology (RSM) to obtain optimum conditions of the reaction variables.
- Rate data analysis based on homogeneous and heterogeneous approach.

- Comparison of experimental data with calculated values obtained from proposed reaction models to check the validity of the model.

It is believed that the data generated in present study will be useful for the rational design of reactors.

CHAPTER 2

Experimental Section

The experimental section is divided into the following parts:

- (a) Catalyst ($TS - 1$) preparation
- (b) Experimental set up
- (c) Procedure
- (d) Analysis of products

Chemicals:

Chemicals used in the present study for the preparation of $TS - 1$ are

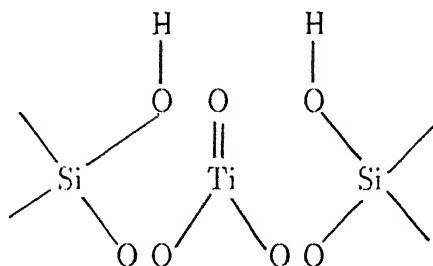
1. Tetraethyl orthosilicate (TEOS)
2. Tetrabutyl orthotitanate ($Ti(OBu)_4$)
3. Tetrapropyl ammonium hydroxide (TPAOH)
4. Iso-propanol

All these chemicals were supplied by M/s.E. Merck (India), Bombay and were of 99.5% purity.

n-Hexane (HPLC solvent), hydrogen peroxide (30 wt%) and acetone (analytical grade), used for *n*-hexane studies were supplied by M/s. E.Merck (India), Bombay, and a purity of 99.5% was assured.

2.1 Catalyst preparation:

In the present study the isomorphous substitution of titanium is performed by replacing aluminium in MFI zeolite structure. The structure of the catalyst *TS* - 1 formed is represented as follows:



Preparation of gel and subsequent crystallization is carried out as follows. It is important to maintain the correct sequence of addition of chemicals to obtain gel of right composition.

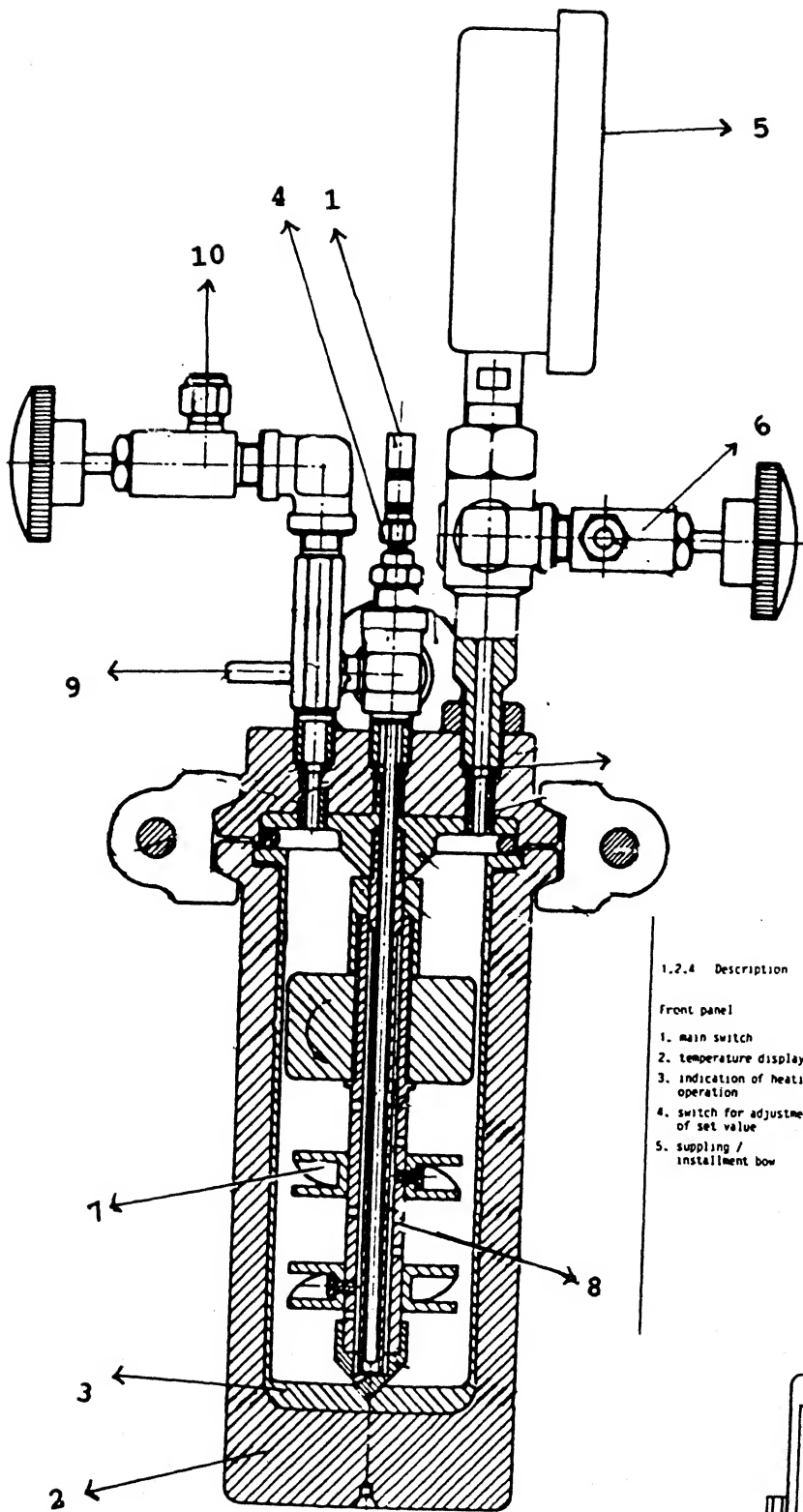
45g (48.3ml) of tetraethyl orthosilicate was taken in a 500ml capacity teflon beaker and stirred using a magnetic stirrer. Then 70g (70ml) of 20 wt% TPAOH was added initially drop by drop and after 10 min at a relatively faster rate under constant stirring. This helps in the complete hydrolysis of TEOS. Heat is generated which helps in the liberation of ethanol. To the clear solution obtained, 2.2g (2.2ml) of $Ti(OBu)_4$ dissolved in 10g (12.8ml) of iso-propanol is added drop by drop under vigorous stirring. Iso-propanol helps in keeping the Ti^{4+} ions in unstable state which helps in better isomorphous substitution of titanium in the catalyst. It is important to get a clear solution after addition of $Ti(OBu)_4$ solution. In case the solution precipitates, the addition of $Ti(OBu)_4$ is stopped until a clear solution is obtained and then the addition of $Ti(OBu)_4$ is resumed. The mixture was kept under stirring for 30 min. It was kept in a water bath at 373K for 30 min to ensure complete evaporation of iso-propanol. 70g (70ml) of double distilled water was added to the resultant mixture and stirred for 15 min.

The final mixture was then poured in a 250 ml teflon lined reactor (Berghof, Germany) and crystallized under autogeneous pressure at a temperature of 443 K under static/stirring conditions for 24 hrs. The resultant gel obtained after reaction was washed, filtered and dried at 373 K for 6 hrs. It was then calcined at 823 K for 12 hrs to remove the template to obtain *TS* - 1 catalyst.

2.2 Experimental setup:

Catalytic activity of *TS*-1 catalyst was studied for liquid phase oxidation of *n*-hexane. The oxidation of *n*-hexane was carried out in a teflon autoclave of 250 ml capacity (Berghof, West Germany) as shown in Fig 2.1. The pressure vessel as well as the lid and all fittings were made of special stainless steel and lined with teflon.

The reaction temperature was measured by means of a teflon covered Ni-Cr/Ni-thermocouple. This thermocouple was connected to a BTR 841 controller with a temperature range of 0-300°C accuracy. The autoclave has the arrangement of withdrawal of gas and liquid sample and a piezo-resistant pressure measuring device with digital display was used to measure pressure in the autoclave. The autoclave contents were stirred with a teflon stirring shaft, which was fitted with a teflon stirring wing and a teflon covered rotor. The shaft was driven by the rotor with a separate stirring motor from the outside. It was connected to a separate control system by which can be adjusted the required speed (200-2000 rpm) with a presetting switch. The valve for liquid sample was marked. The teflon tube of the liquid sample device with the stirring shaft reaches the bottom of the teflon beaker liner. The liquid sample was drawn under pressure by opening of the valve meant for liquid.

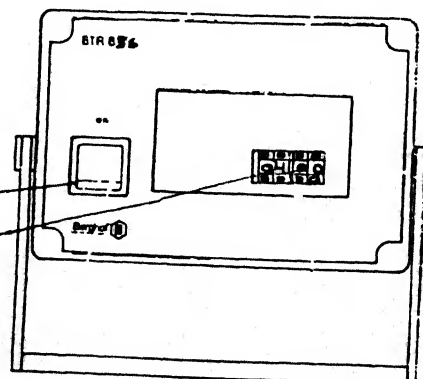
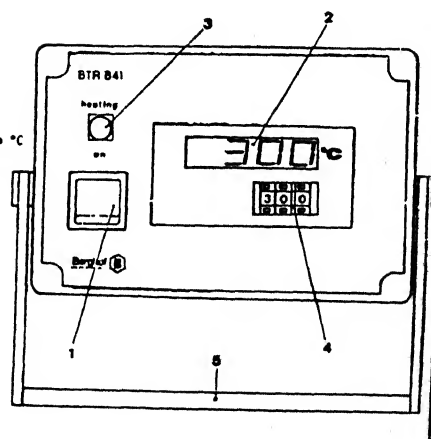


1. Thermocouple, PTFE covered ready to be screwed in.
2. Pressure vessel
3. PTFE liner
4. Thermocouple adapter
5. Pressure gauge
6. Regulating valve
7. Stirring wing
8. Stirrer shaft
9. Liquid sample extraction device
10. Gas sample extraction device

1.2.4 Description

Front panel

1. main switch
2. temperature display in °C
3. indication of heating operation
4. switch for adjustment of set value
5. supplying / installment bow



main switch

switch for adjustment
of set value

2.3 Experimental procedure:

2.3.1 Kinetic study:

The kinetic data were obtained at different reaction temperatures ranging from 353 to 393K on *TS* - 1 catalyst at different reaction times ranging from 3-12 hrs.

In all the experiments, the catalyst was dispersed in 30 wt% hydrogen peroxide, overnight, so that peroxy sites, which are the oxygen donors for oxidation of *n*-hexane, were formed on the catalyst. This was verified by the disappearance of 960 cm^{-1} infra red band attributed to titanyl group in the catalyst or the change in colour of the catalyst from white to yellow. 13.33g (20ml) of *n*-hexane and 23.7 g (30 ml) of acetone were added to 4.165 g (3.8 ml) of 30wt% hydrogen peroxide. Acetone was used as a solvent to increase the solubilities of *n*-hexane and hydrogen peroxide. To this mixture 0.2g of *TS* - 1 catalyst was added. The mixture was stirred under autogeneous pressure at a speed of 400 rpm at the required temperature. Samples were collected at different times with the help of liquid drawing valve.

2.3.2 Optimization studies:

After obtaining the kinetic data at various temperatures and times, the main variables affecting the reaction were found out. In the oxidation of *n*-hexane, the important variables are reaction temperature, reaction time, catalyst loading (*gm* catalyst/*gm**n*-hexane) and hydrogen peroxide/*n*-hexane mole ratio. Since there are four independent parameters, 2^4 design of experiments were conducted around the assumed base levels and the conditions for getting maximum yield were optimized.

2.4 Product analysis:

The liquid samples were analysed in a GGC gas chromatograph supplied by M/s Chromatography and Instruments Company, Baroda. The chromatograph was fitted with a flame ionisation detector (FID). The column temperature was kept at 373K whereas the injection temperature was maintained at 418 K. The flow rates of nitrogen and hydrogen were kept at 35 ml/min. To separate the components of the reaction product, a 3mm OD x 2.4m long stainless steel column packed with 5% Carbowax 20M on Chromosorb-W.H.P of 80-100 mesh size was used. The column separated *n*-hexane, acetone, hexanol and hexanone effectively. A typical chromatogram is shown in Fig 2.2.

2.4.1 Calibration:

The chromatograph was calibrated using a mixture of known composition, and retention times were obtained. The following are the retention times under the operating conditions:

n-hexane = 35 sec

hexanol = 45 sec

hexanone = 55 sec

To get quantitative results from the measured peak areas, certain correction factors known as 'response factors' were used before normalizing the areas for calculating the percentage composition. The following response factors were available in the literature (Dietz 1967, Shingari 1988).

n-hexane = 0.7

hexanol = 1.02

hexanone = 0.74

These are independent of temperature, carrier gas, flow rate and concentration (Dietz 1967). Area under any peak divided by the response factor gives its true area. Normalizing these true areas will give mole fractions of different components present.

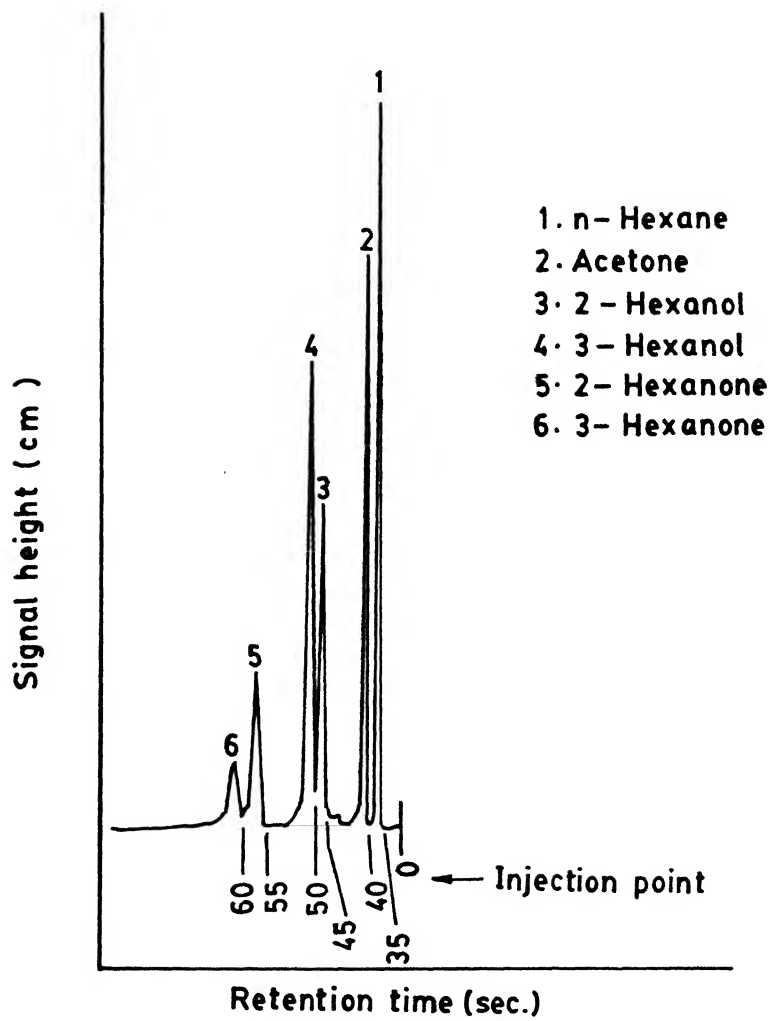


Fig 2.2 A Typical Chromatogram

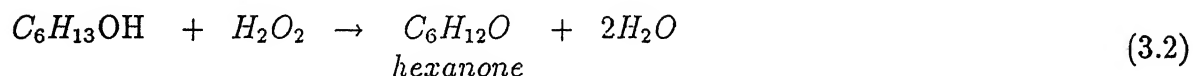
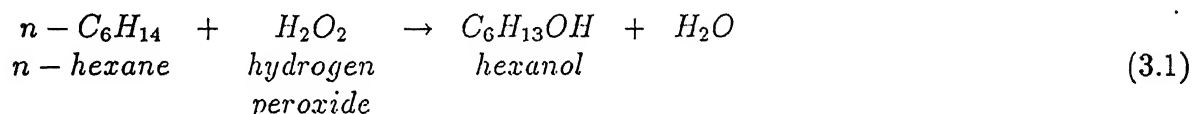
CHAPTER 3

REACTION MODELLING

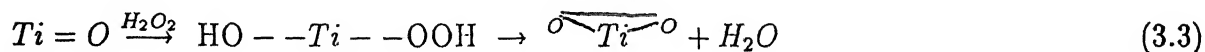
Reaction modelling and kinetic data analysis help in better understanding of reaction mechanism and identification of important reaction parameters useful for the design of reactors.

3.1 Reaction Mechanism :

Oxidation of *n*-hexane with hydrogen peroxide is represented as :



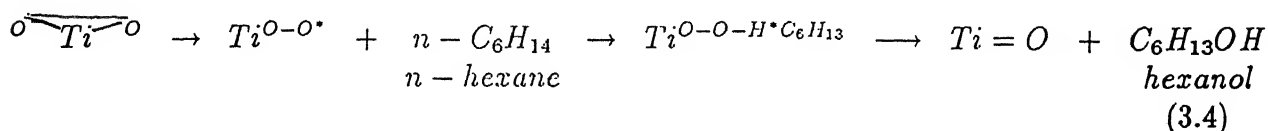
In the above oxidation reaction 2-hexanol and 3-hexanol are formed beside 2-hexanone and 3-hexanone. In the present study 2-hexanol and 3-hexanol were treated as total hexanol. Similarly 2 and 3-hexanones were taken as total hexanone. In the oxyfunctionalization of *n*-hexane, oxidation occurs selectively at the tertiary *C* – *H* bond. The surface titanyl group (*Ti* = *O*) is the basic unit of active sites present in *TS* – 1 catalyst. Hydroxyhydroperoxo or peroxo complexes formed on the titanyl group by reaction with hydrogen peroxide are the oxygen donors. The FORMation of such complexes is represented in equation (3.3).



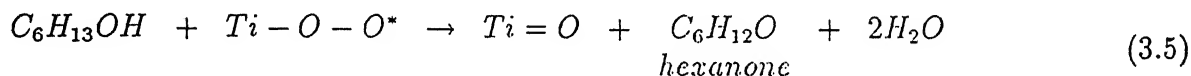
Evidence for the formation of peroxo complexes is found by absorption of hydrogen peroxide on *TS* – 1 catalyst followed by vacuum drying. This treatment causes the disappearance of 960cm^{-1} infra red band, ascribed to surface titanyl group. This absorption is characteristic for titanium complexes with peroxo ligands. Heating of the hydrogen

peroxide treated $TS - 1$ leads to decomposition of the titanium peroxocomplexes with re-formation of titanyl group (960cm^{-1} absorption band reappears). The change of colour from white to yellow of the $TS - 1$ catalyst is also an indication for the formation of peroxo complexes.

Considering the inertness of the saturated hydrocarbons, n -hexane oxidation requires a homolytic mechanism giving rise to radical intermediates. Such mechanism is represented in equation (3.4). The reactivity of titanium peroxo complex is attributed to the generation of an open diradical form, followed by hydrogen abstraction from n -hexane to give a carbon diradical. Recombination with the hydroxyl radical from $Ti - O - OH$ yields the hexanol and the titanyl group.



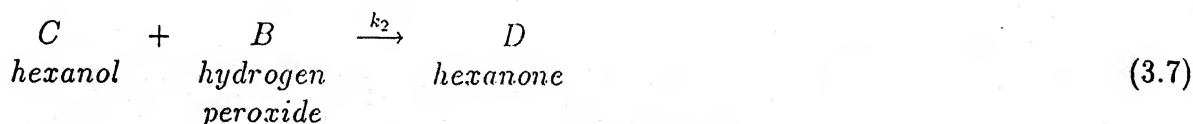
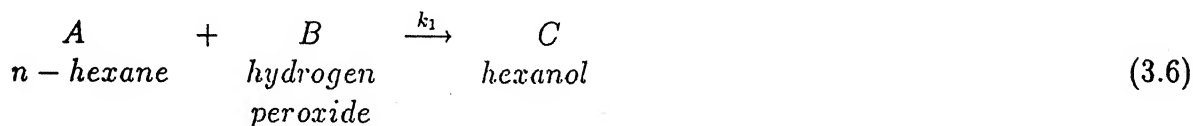
Following the same mechanism hexanol is converted to hexanone as shown in the equation (3.5).



3.2 Reaction Modeling

3.2.1 Homogeneous model:

In the solid-liquid reactions, if diffusion is not controlling the rate of reaction, then, homogeneous model can be used to represent the reaction between n -hexane and hydrogen peroxide. The reaction is represented by equations (3.6) and (3.7).



$$\text{Rate of } n\text{-hexane disappearance} = -r_A = dC_A/dt = k_1 C_A C_B, \quad \text{gmol/cc-sec} \quad (3.8)$$

$$\text{Rate of } H_2O_2 \text{ disappearance} = -r_B = dC_B/dt = k_1 C_A C_B + k_2 C_B C_C, \quad \text{gmol/cc-sec} \quad (3.9)$$

$$\text{Rate of formation of hexanol} = r_C = dC_C/dt = k_1 C_A C_B - k_2 C_B C_C, \quad \text{gmol/cc-sec} \quad (3.10)$$

$$\text{Rate of formation of hexanone} = r_D = dC_D/dt = k_2 C_B C_C, \quad \text{gmol/cc-sec} \quad (3.11)$$

The concentrations of various components are related to concentration of A as follows:

$$\text{Concentration of } n\text{-hexane } C_A = C_{A0}(1 - X_A) \quad (3.12)$$

$$\text{Concentration of } H_2O_2 \text{ } C_B = C_{A0}(M - X_A) \quad (3.13)$$

Concentration of hexanol, C_C , is given by equation (3.14) (Levenspiel, 1989),

$$\text{Concentration of hexanol } C_C = \frac{k_1 C_A}{k_1 - k_2} \left[\left\{ \frac{C_{A0}}{C_A} \right\}^{1-(k_2/k_1)} - 1 \right] \quad (3.14)$$

$$\text{Concentration of hexanone } C_D = C_T - C_{A0}(1 - X_A) - C_C \quad (3.15)$$

M = Initial mole ratio of H_2O_2 to n -hexane.

X_A = Fractional conversion of n -hexane.

C_{A0} = Initial concentration of n -hexane, gmol/cc

C_T = Total concentration on product side, gmol/cc

The rate constants k_1 and k_2 as given in equations (3.12) to (3.15) can be obtained by linear regression (Gupta, S.K., 1992) by minimizing the objective function defined as:

$$S = \sum_{i=1}^n [(r_A)_{\text{expt}} - (r_A)_{\text{calc}}]^2 \quad (3.16)$$

where, n = no of data points

$(r_A)_{\text{expt}}$ = experimental rate of n -heane, gmol/cc - sec

$(r_A)_{\text{calc}}$ = calculated rate of n -hexane, gmol/cc - sec

The conversion, yield and selectivities (both experimental and calculated) are defined as follows:

$$\% \text{Conversion of } n\text{-hexane}, (X_A)_{\text{expt}} = \frac{\text{Moles of } n\text{-hexane converted} \times 100}{\text{Moles of } n\text{-hexane fed}}, \quad (3.17)$$

$$\% \text{Yield of (hexanol+hexanone)}, Y_{\text{expt}} = \frac{\text{Moles of hexanol} + \text{hexanone} \times 100}{\text{Moles of } n\text{-hexane fed}}, \quad (3.18)$$

$$\% \text{Selectivity of hexanol}, (S_1)_{\text{expt}} = \frac{\text{Moles of hexanol} \times 100}{\text{Moles of hexanol} + \text{hexanone}}, \quad (3.19)$$

$$\% \text{Selectivity of hexanone}, (S_2)_{\text{expt}} = (100 - S_1) \quad (3.20)$$

It has been assumed that only two products hexanol and hexanone are formed from the reaction. Once the rate constants are evaluated, it is possible to calculate the rates from the equations (3.8) to (3.11) as follows:

$$(r_A)_{\text{calc}} = k_1(C_{A0}^2(X_A^2)_{\text{calc}} - (M+1)(X_A)_{\text{calc}} + M) \quad (3.21)$$

Only $-ve$ part of the discriminant is taken in the above equation since $+ve$ part gives a conversion of more than 100% which is not possible.

M = Initial mole ratio of H_2O_2 to n -hexane

$$(C_C)_{\text{calc}} = \frac{k_1 C_{A0} \{1 - (X_A)_{\text{calc}}\}}{k_1 - k_2} \left[\left\{ \frac{1}{1 - (X_A)_{\text{calc}}} \right\}^{(1 - k_2/k_1)} - 1 \right] \quad (3.22)$$

$$(C_D)_{\text{calc}} = C_T - C_{A0}(1 - (X_A)_{\text{calc}}) - (C_C)_{\text{calc}} \quad (3.23)$$

Similarly yield Y and selectivities S_1 and S_2 are also calculated from equations (3.19) to (3.21). These values are compared with the experimental values.

$$Y_{\text{calc}} = \frac{(C_C)_{\text{calc}} + (C_D)_{\text{calc}} \times 100}{C_{A0}} \quad (3.24)$$

$$(S_1)_{\text{calc}} = \frac{(C_C)_{\text{calc}} \times 100}{(C_C)_{\text{calc}} + (C_D)_{\text{calc}}} \quad (3.25)$$

$$(S_2)_{\text{calc}} = (100 - (S_1)_{\text{calc}}) \quad (3.26)$$

Effect of reaction temperature over the reaction rate constants k_1 and k_2 can be evaluated from Arrhenius equations (3.28) and (3.29). $\ln k_1$ and $\ln k_2$ are plotted against reciprocal of reaction temperature to obtain the values of activation energies from the slopes of these plots.

$$k_1 = k_{10} \exp(-E/RT) \quad (3.27)$$

$$k_2 = k_{20} \exp(-E/RT) \quad (3.28)$$

k_1, k_2 are homogeneous reaction rate constants, $\text{gmol/cc} - \text{sec}$

k_{10}, k_{20} are preexponential factors

3.2.2 Heterogeneous Model:

The oxidation of *n*-hexane is carried out in the presence of solid catalyst *TS* – 1. *TS* – 1 is a titanium silicalite porous catalyst where titanium sites active for oxidation reactions are present in the silicalite structure. Therefore, the reaction system cannot be treated as homogeneous one but rather heterogeneous approach in the analysis of kinetic data should also be attempted. In the heterogeneous model, the reaction takes place on the surface sites. Diffusion plays an important role in the reaction. Diffusion of reactants and products is assumed to be fast as compared to the reaction.

In the case of heterogeneous model Langmuir - Hinshelwood-Hougen-Watson (LHHW) approach is used to develop kinetic model. This approach consists of three steps:

- 1) Adsorption of reactants on catalyst surface
- 2) Surface reaction to give products
- 3) Desorption of products from the surface of the catalyst

In heterogeneous reaction mechanism, adsorption, surface reaction and desorption govern the rate of reaction.

Generally one of the above three steps control the reaction rate. In LHHW approach, two types of mechanisms are possible.

- 1) Single site mechanism
- 2) Dual site mechanism

1. Single site mechanism:

In the case of single site mechanism the reaction takes place as follows:

Hydrogen peroxide was absorbed on *TS* – 1 to form peroxy sites which react with *n*-hexane to give an intermediate of hexanol and a vacant site of *TS* – 1. This peroxy site further reacts with hexanol to give the intermediate of hexanone which in turn desorbs to give hexanone.



2. Dual site mechanism:

In the case of dual site mechanism the following reaction takes place:

n-Hexane and hydrogen peroxide adsorb on *TS* - 1. These two adsorbed sites react to give intermediate of hexanol. This intermediate desorbs to give hexanol. Again the hexanol reacts with the peroxy site of *TS* - 1 to form an intermediate of hexanone which in turn desorbs to give hexanone.



Table 3.1: Rate Expressions based on different mechanisms

| Mechanism | Controlling step | Rate expression |
|-------------|---------------------------|---|
| Single site | Adsorption of B | $r_A = \frac{k_A C_B}{1 + \frac{K_{D1} C_C}{K_{sr1} C_A} + K_{D1} C_C + K_{D2} C_D}$ |
| | Surface reaction of A & C | $r_{sr} = \frac{k_{sr1} C_A C_B + k_{sr2} C_B C_C}{\frac{1}{K_A} + C_B + \frac{K_{D1} C_C}{K_A} + \frac{K_{D2} C_D}{K_A}}$ |
| | Desorption of C & D | $r_D = \frac{K_A C_B (k_{D1} K_{sr1} C_A + k_{D2} K_{sr2} C_C)}{\{1 + K_A C_B (1 + K_{sr1} C_B + K_{sr2} C_C)\}}$ |
| Dual site | Adsorption of A & B | $r_A = \frac{k_{A1} C_A + k_{A2} C_B}{1 + \frac{K_{D2} K_{sr1}}{K_{sr2}} C_D + \frac{K_{sr2} K_{D1}}{K_{D2}} \frac{C_C}{C_D} + K_{D1} C_C + K_{D2} C_D}$ |
| | Surface reaction of A & C | $r_{sr} = \frac{k_{sr1} K_{A1} K_{A2} C_A C_B + k_{sr2} K_{D1} K_{A2} C_B C_C}{(1 + K_{A1} C_A + K_{A2} C_B + K_{D1} C_C + K_{D2} C_D)^2}$ |
| | Desorption of C & D | $r_D = \frac{K_{sr1} K_{A1} K_{A2} C_A C_B (k_{D1} + k_{D2} K_{sr2} C_B)}{1 + K_{A1} C_A + K_{A2} C_B + K_{sr1} K_{A1} K_{A2} C_A C_B (1 + K_{sr2} C_B)}$ |



Different rate expressions for the above type of reactions are given (Froment and Bischoff, Fogler, 1992) in Table (3.1): K_A , K_{A2} , K_{D1} , K_{D2} are adsorption and desorption constants, $\frac{cc}{gmol-gcat}$

K_{sr1}, K_{sr2} are surface reaction equilibrium constants, gmol/gcat–sec

C_A, C_B, C_C, C_D are the concentrations of *n*-hexane(A), hydrogen peroxide(B), hexanol(C) and hexanone(D), gmol/cc.

The various rate expressions presented in Table 3.1 are nonlinear in nature. To estimate the reaction parameters, a non-linear algorithm known as Rosen Brock optimization technique can be used. In this technique the objective function is defined in equation (3.16) as:

$$S = \sum_{i=1}^n [(r_{\text{exp}} - r_{\text{calc}})]^2$$

where, n is no of data points

r_{exp} is experimental rate, gmol/gcat–sec

r_{calc} is calculated rate, gmol/gcat–sec

The parameters can be estimated by minimizing the objective function. The initial guess values of the parameters are obtained by linearizing the rate expression. Effect of reaction temperature over these parameters is accounted by Arrhenius equation.

From the rate controlling step equation $(X_A)_{\text{calc}}$ is calculated from which the theoretical concentrations of A, B, C and D are calculated. The theoretical yield and selectivities are calculated according to the equations (3.24) to (3.26).

The surface reaction rate constants, adsorption and desorption constants are related with reaction temperature as follows:

$$k_{sr1} = k_{sr1o} \exp(-E/RT) \quad (3.40)$$

$$k_{sr2} = k_{sr2o} \exp(-E/RT) \quad (3.41)$$

$$K_{A1} = K_{A1o} \exp(-\Delta H_{A1}/RT) \quad (3.42)$$

$$K_{A2} = K_{A2o} \exp(-\Delta H_{A2}/RT) \quad (3.43)$$

$$K_{D1} = K_{D1o} \exp(-\Delta H_{D1}/RT) \quad (3.44)$$

$$K_{D2} = K_{D2o} \exp(-\Delta H_{D2}/RT) \quad (3.45)$$

where,

ΔH_A = heat of adsorption of H_2O_2 , kcal/gmol

ΔH_{D1} = heat of desorption of hexanol, kcal/gmol

ΔH_{D2} = heat of desorption of hexanone, kcal/gmol

E = apparent activation energy, kcal/gmol

k_{sr1o}, k_{sr2o} (gmol/gcat-sec), K_{Ao}, K_{D1o}, K_{D2o} (cc/gmol-gcat), are pre exponential factors, cc/gmol.

Once the rate parameters are calculated from LHHW model, the reaction rates can be calculated. From the calculated rates, conversion, yield and selectivities are calculated from equations (3.22) to (3.27).

The experimental conversion, yield and selectivities are compared with calculated ones. This further validates the accuracy of the reaction models proposed.

3.3 OPTIMIZATION STUDIES :

In the present investigation, it is important to determine and quantify the relationship between the yield of (hexanol + hexanone) over $TS-1$ catalyst and the settings of the independent variables (reaction temperature, reaction time, gm catalyst/gmn-hexane and H_2O_2 /n-hexane mole ratio). These variables affect the yield of (hexanol + hexanone). One of the other aims is to find the settings of the experimental factors that produce the best yield of (hexanol + hexanone). These investigations are done using design of experiments combined with Response Surface Methodology (RSM). The effect of the above experimental factors on the conversion of n-hexane and the selectivity towards hexanol and hexanone are also determined. A brief introduction to response surface methodology is given below (Draper, N.R. et al., 1981).

3.3.1 Response Surface Methodology:

Let Y be the response of a chemical process dependent on the levels of k factors x_1, x_2, \dots, x_k which can be precisely measured and controlled. The model for the u^{th} combination of factor levels is given by,

$$Y_u = f(x_{1u}, x_{2u}, \dots, x_{ku}) + e_u, u = 1, 2, \dots, N \quad (3.46)$$

where N is the number of experiments,

f : the functional relationship,

e : the error involved.

A geometrical portrait of the response function in the factor space is called a response surface.

The experimental region R , is a bounded subspace of the whole factor space. The experimental region is bounded because of the practical limitations. The response surface methodology deals with the problem of locating a point $(x_1^0, x_2^0, \dots, x_k^0)$ within the experimental region R , at which Y is an extremum (Box, G.E.P. et al., 1955; Cochran, W.G. et al., 1957; Davis, O.L. et al., 1956; Hill, W.J. et al., 1966). The response surface methodology, originally introduced by Box and Wilson (Box, G.E.P. et al., 1951), is essentially applied in two stages in order to find the optimum conditions. The two stages are termed the first-order strategy and the second-order strategy respectively. The methodology is applied as follows :

The first step is to design a set of experiments and conduct them to get reliable estimates of the parameters, called factorial design. The details of the factorial design are discussed by Box et al. (1978). The second step in using the response surface methodology is to propose a suitable mathematical model to fit the experimental data and then test for model adequacy through a lack-of-fit F test (Draper, N.R. et al., 1981). The third and the last step is to find out the optimum conditions of the independent variables which will produce the maximum (or minimum) value of the response.

The conventional one factor-at-a time method, where the experiments are conducted holding all the other factors constant often fails to locate the true optimum. The response surface methodology cuts down experimental effort by making use of experimental designs which permit the experimenter to assess the strengths of the interactions between the factors while varying them simultaneously.

RSM is sequential in nature. Some experiments are carried out, valuable information is gathered and the next stage is designed for getting better values of the response. Generally the method of steepest ascent (or descent) is applied for moving sequentially along the direction of maximum (or minimum) increase (or decrease) in response.

3.3.2 First Move on the Response Surface :

1. Identification of Variables and their Response

Important variables which influence the oxidation of *n*-hexane to hexanol and hexanone are the reaction temperature, reaction time, *gm* catalyst/*gmn*-hexane and H_2O_2/n -hexane mole ratio. After knowing the important variables influencing the progress, a base level had to be chosen within the experimental region. The base levels of the factors were chosen on the basis of an a-priori knowledge. Further the variation interval for each factor had to be chosen. The variation interval of a factor when added or subtracted from the base level gives the upper or lower level of the factor respectively.

To simplify the recording of the conditions of an experiment, and the processing of the experimental data the values of the factors were coded as follows:

$$x_i = \frac{\bar{x}_i - \bar{x}_{i0}}{v_i} \quad i = 1, 2, \dots, k \quad (3.47)$$

where x_i is the coded value of the *i*-th factor,

\bar{x}_i is the natural value of the *i*-th factor,

\bar{x}_{i0} is the natural value of the base level of the *i*-th factor,

and v_i is the variation interval of the *i*-th factor.

Conventionally, the coded value of the upper level corresponds to +1, the lower level to -1 and the base level to 0.

2. Identification of the Optimization Parameters:

The following dependent variables (responses) are considered to be important:

- a) Conversion of *n*-hexane,
- b) Yield towards hexanol + hexanone,
- c) Selectivity of hexanol and hexanone.

Of the above responses, the yield of (hexanol + hexanone) is selected as the response to be optimized with respect to the independent variables. Though the conversion of *n*-hexane and the selectivities of hexanol and hexanone are not optimized, data for these two responses are also processed and fitted to models to quantify the relationship with the settings of a group of experimental factors.

3. Selection of Experimental Design:

Since there are four independent variables, a 2^4 factorial design around the base levels were employed in the present study. Experiments were carried out in a randomized sequence to avoid bias on the part of experimenter. The values of all the responses (conversion, yield and selectivities) for the first move are calculated. One of the design experiments was repeated to get the estimate of the pure error.

4. Model Fitting:

The following first order model has been fitted to the experimental data.

$$\hat{Y} = \hat{b}_0 + \hat{b}_1x_1 + \hat{b}_2x_2 + \hat{b}_3x_3 + \hat{b}_4x_4 \quad (3.48)$$

where $\hat{b}_0, \hat{b}_1, \hat{b}_2, \hat{b}_3, \hat{b}_4$ are the best fitted values of coefficients, x_i is the *i*-th variable of its coded form and \hat{Y} is the predicted values of the response. The coefficients can be estimated by the least square technique as

$$\hat{\underline{b}} = (\underline{X}^T \underline{X})^{-1} \underline{X}^T \underline{Y} \quad (3.49)$$

where \underline{X} is the design matrix, \underline{X}^T is the response of the design matrix, \underline{Y} is the vector of responses and $\hat{\underline{b}}$ the vector of coefficients. The details of the method are given by Draper and Smith (1981). This is then tested for model adequacy by a lack-of-fit *F* test.

The effect of different variables is evident from the values of the coefficients of the corresponding model. The magnitude of the coefficient represents the amount of change in

the response for the change of variables from the base level to the upper levels. Positiveness of the coefficient indicates the increase in the response with an increase of the variable from the base level to the upper level. Negative sign of the coefficient indicates the same but in the opposite sense.

5. Calculation of the Path of Steepest Ascent and Conduct of Experiments Along this Path:

Information obtained from the models was used to locate the path of maximum increase in yield. The method of steepest ascent is a procedure for moving sequentially along the direction of maximum increase in the response.

The direction of steepest ascent was determined using the relation,

$$\nabla \Phi = \frac{\delta \Phi}{\delta x_1} \bar{u}_1 + \frac{\delta \Phi}{\delta x_2} \bar{u}_2 + \dots + \frac{\delta \Phi}{\delta x_k} \bar{u}_k \quad (3.50)$$

where Φ is the function describing the response surface,

$\nabla \Phi$ is the gradient of the response function,

$\frac{\delta \Phi}{\delta x_i}$ is the partial derivative of the function with respect to the i -th factor,

$\bar{u}_1, \bar{u}_2, \dots, \bar{u}_k$ are the unit vectors in the direction of the co-ordinate axes.

It can be easily verified that the components of the

gradient $\nabla \Phi$ i.e., $\frac{\delta \Phi}{\delta x_i} (i = 1, 2, \dots, k)$ are same as the

regression coefficient as in Equation (3.49). Thus by changing the independent variables x_1, x_2, x_3 and x_4 in proportion to the values of their corresponding coefficients, the movement along the steepest path may be realised which gives the optimum conditions for maximum yield.

CHAPTER 4

RESULTS AND DISCUSSION

Oxidation of *n*-hexane with 30wt% hydrogen peroxide was carried out using *TS* - 1 catalyst in a batch reactor. Effect of important variables like reaction temperature, reaction time, % catalyst loading (gm cat/*gm n*-hexane $\times 100$) and hydrogen peroxide/*n*-hexane mole ratio on the conversion of *n*-hexane, yield of (hexanol + hexanone), selectivities of hexanol and hexanone were studied. The experimental range of variables in the present study are given in Table 4.1.

Table 4.1 Reaction Variables and their range

| Variable | Range |
|------------------------------------|---------------|
| Reaction temperature | 353 – 393K |
| Reaction time | 3 - 12 hours |
| % Catalyst loading | 1.5 – 3% |
| H_2O_2/n -hexane mole ratio | 0.2 - 1.0 |
| $\frac{T_i}{(S_i+T_i)}$ mole ratio | 0.025 - 0.035 |

All the experiments were carried in a batch reactor under autogeneous pressure. Conversion, yield and selectivity were defined as follows:

$$\% \text{ Conversion of } n\text{-hexane} = \frac{\text{Moles of } n\text{-hexane converted} \times 100}{\text{Initial moles of } n\text{-hexane fed}}$$

$$\% \text{ Yield of (hexanol+hexanone)} = \frac{\text{Moles of (hexanol+hexanone)} \times 100}{\text{Initial moles of } n\text{-hexane fed}}$$

$$\% \text{ Selectivity of hexanol} = \frac{\text{Moles of hexanol in product} \times 100}{\text{Moles of (hexanol + hexanone)}}$$

$$\% \text{ Selectivity of hexanone} = \frac{\text{Moles of hexanone in product} \times 100}{\text{Moles of (hexanol + hexanone)}}$$

4.1 Reproducibility of Kinetic Data:

Reproducibility of kinetic data was tested by repeating the experimental runs under identical conditions and finding the experimental error. All the runs were conducted for 8 hours, a % catalyst loading of 1.5% and H_2O_2/n -hexane mole ratio of 0.2. The experiments were conducted using $TS-1$ as catalyst. The conversion of n -hexane was found to increase continuously until 393 K. Fig.4.1 represents a typical data of 3 experimental runs conducted under identical conditions. Table 4.2 gives the values of n -hexane conversion.

Table 4.2 n -hexane conversion(%) data over $TS-1$ catalyst (Reproducibility data)

| Run/Temperature (K) | 353 | 363 | 373 | 383 | 393 |
|---------------------|-------|-------|-------|-------|-------|
| 1 | 24.2 | 25.31 | 34.08 | 39.23 | 57.21 |
| 2 | 24.53 | 24.92 | 35.1 | 38.78 | 55.9 |
| 3 | 25.6 | 26.1 | 33.83 | 40.3 | 55.83 |

The data was reproducible within an error of 5%.

4.2 Effect of Important Reaction Variables at 4.2.1 Effect of Reaction Temperature:

Effect of reaction temperature on conversion of n -hexane, yield of (hexanol + hexanone) and selectivities of hexanol and hexanone were studied. The effect of temperature on n -hexane conversion is shown in Fig.4.2. The conversion of n -hexane was found to

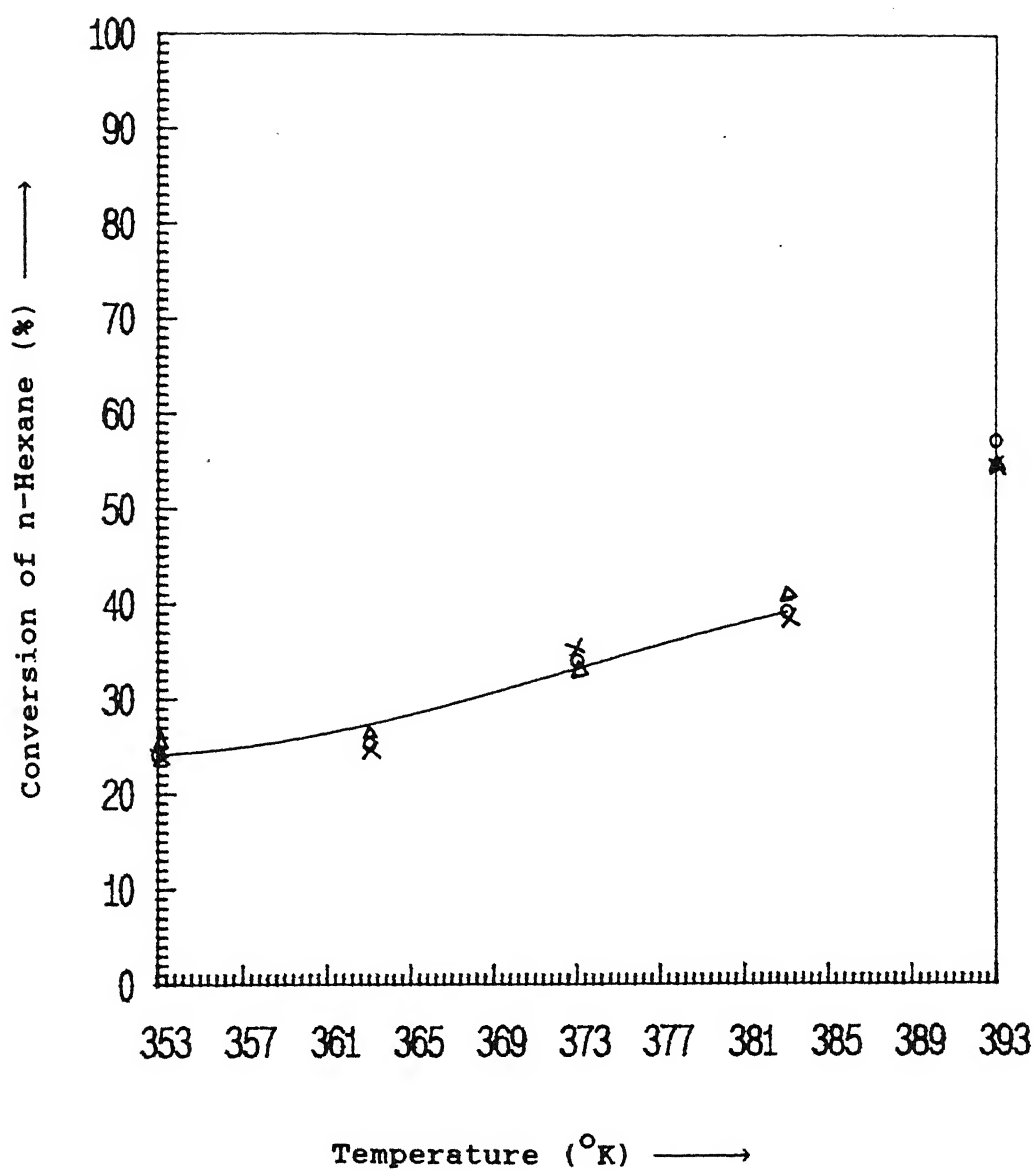


Fig 4.1 Reproducibility of Experimental Data (TS-1Catalyst,
Time = 8 hours, % Catalyst Loading = 1.5,
 $\text{H}_2\text{O}_2/\text{n-hexane}$ Mole Ratio = 0.2)

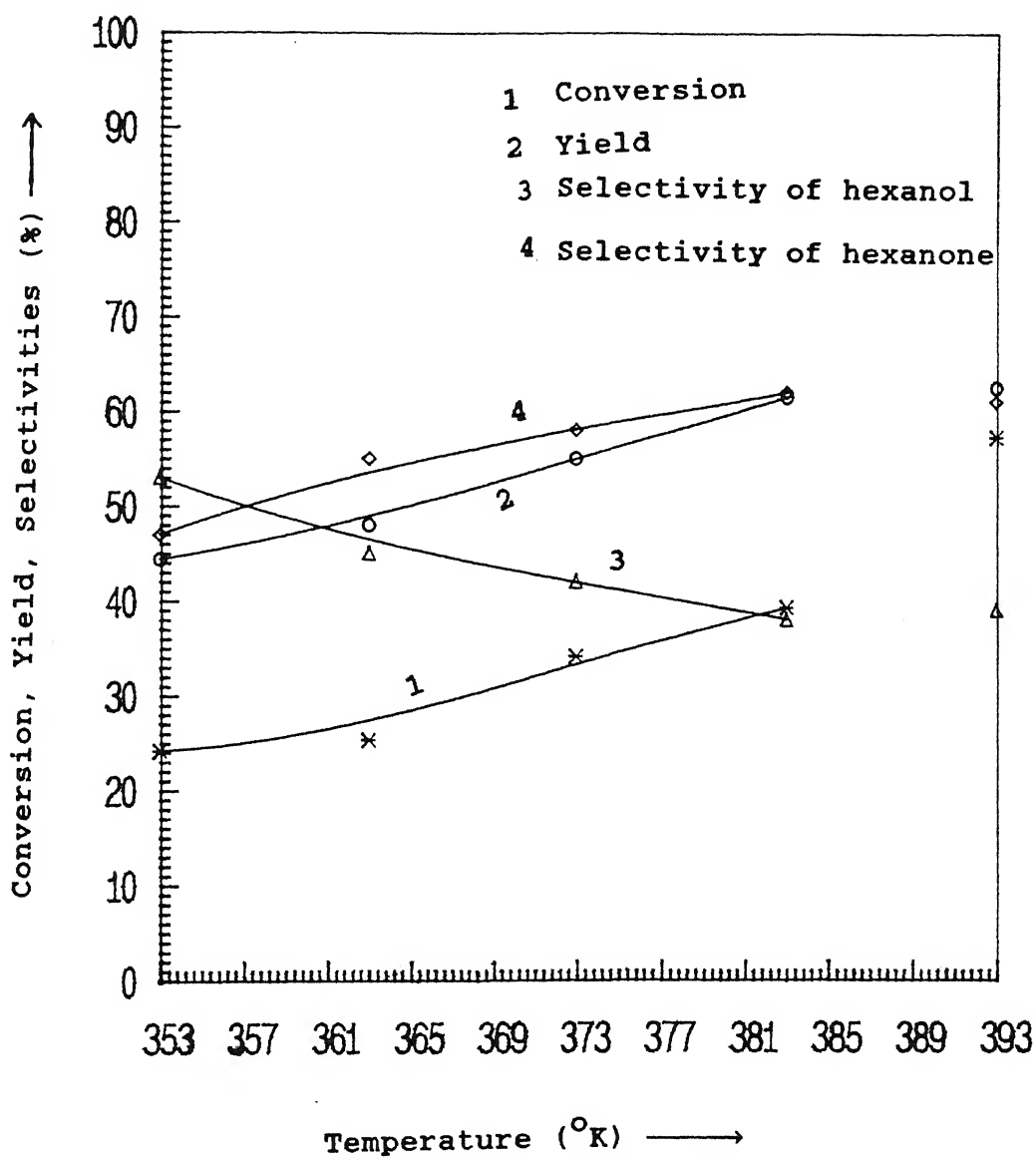


Fig 4.2 Effect of Temperature on n-Hexane Conversion

(TS-1 Catalyst, Time = 8 hours, % Catalyst Loading = 1.5,
 $\text{H}_2\text{O}_2/\text{n-Hexane MoleRatio} = 0.2$)

increase with temperature and it continued until 393 K. At higher temperatures hydrogen peroxide would decompose thus the reaction temperature was limited to 393 K. The yield of (hexanol + hexanone) also increased with increase in temperature. The selectivity of hexanol was found to decrease with increase in reaction temperature while the selectivity of hexanone continuously increased with temperature. This was due to the further reaction of hexanol to form hexanone. Experiments carried out at different temperatures suggested the existence of an optimum temperature for maximum yield of desired product. The hexanol/hexanone ratio was found to decrease with increase in the reaction temperature.

4.2.2 Effect of Reaction Time on Conversion of *n*-Hexane:

The effect of reaction time on the conversion of *n*-hexane over *TS* - 1 catalyst was studied. The range of reaction time varies from 3 - 12 hours. Fig.4.3 shows the effect of reaction time on conversion of *n*-hexane. The conversion increased until a time of 8 hours and remains constant after that. As time increased more and more of *n*-hexane react with hydrogen peroxide and gets converted to hexanol and hexanone. But after 8 hours due to the unavailability of hydrogen peroxide, no more reaction took place and hence the conversion remained constant. This was due to the depletion of hydrogen peroxide to water and oxygen molecules.

Fig.4.4 shows the effect of reaction time on concentration of *n*-hexane. All the curves at different temperatures start at an initial concentration of *n*-hexane 6.51×10^{-3} gmol/cc which was kept constant in all experimental runs. Concentration decreased continuously until 8 hours due to more and more conversion of *n*-hexane and then remained constant.

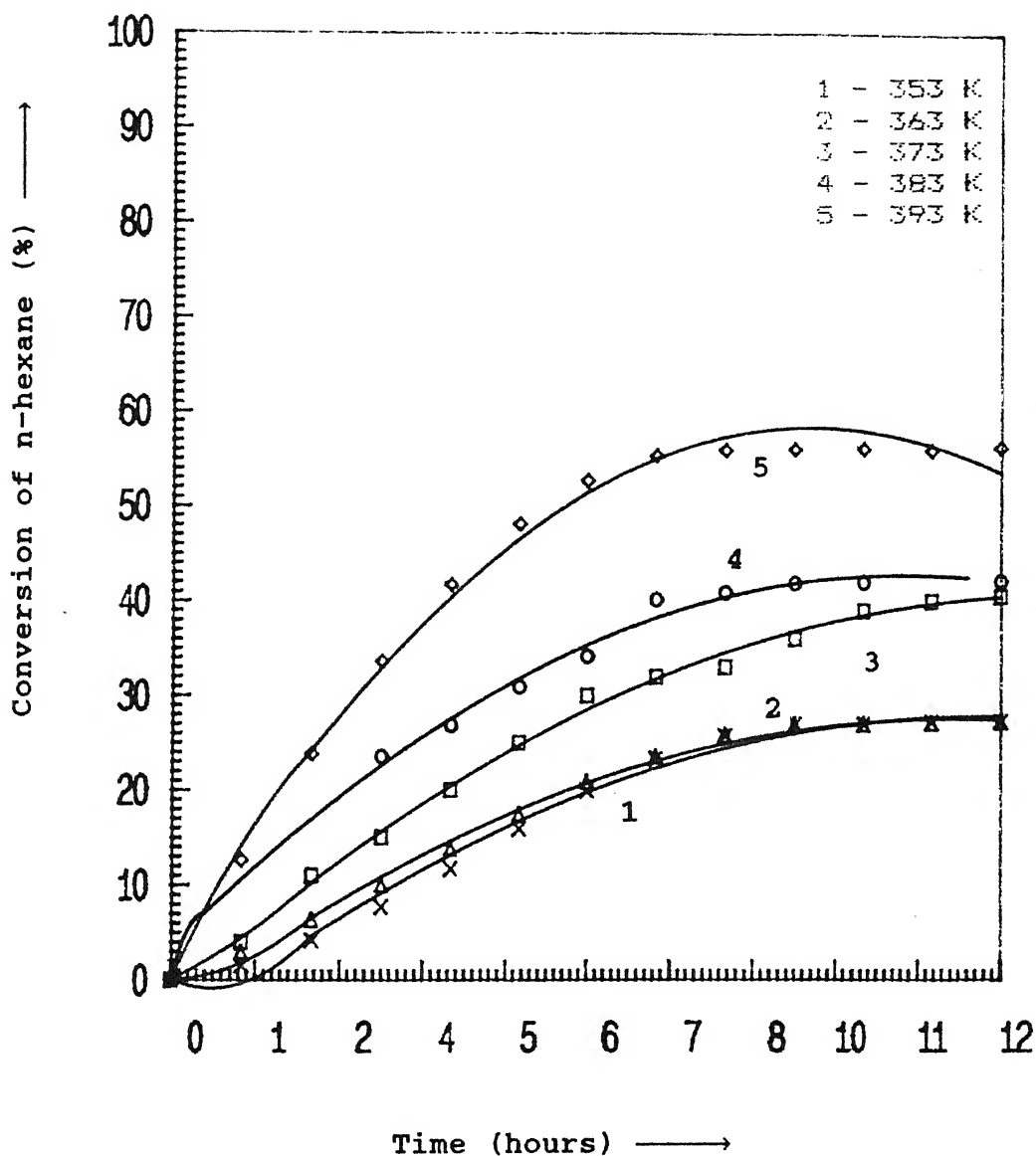


Fig 4.3 Effect of Reaction Time on Conversion of n-Hexane

(TS-1 Catalyst, Temperature = 353- 393 K,

% Catalyst Loading = 1.5, $\text{H}_2\text{O}_2/\text{n-Hexane}$ Mole Ratio = 0.2)

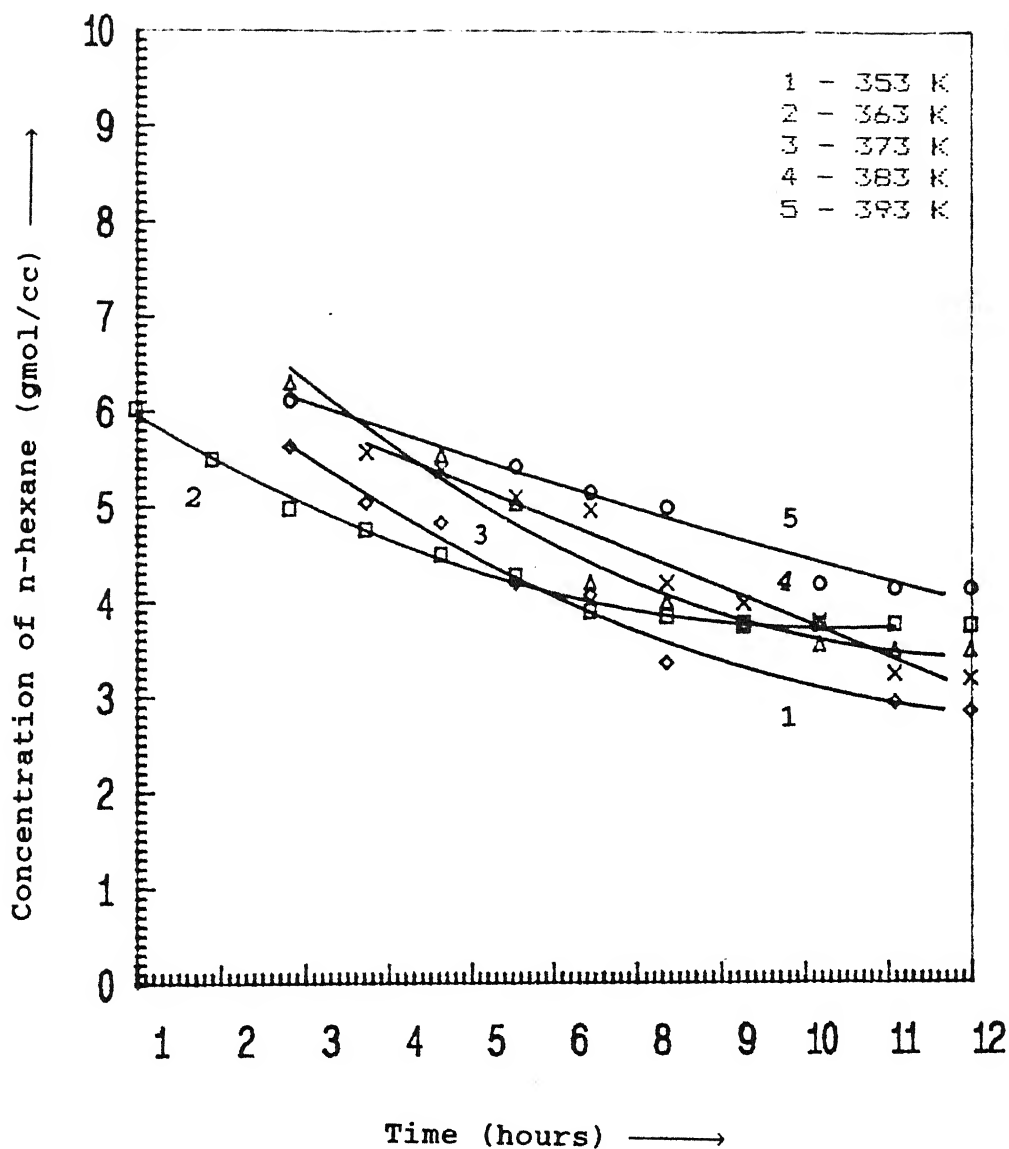


Fig 4.4 Effect of Reaction Time on Concentration of n-Hexane
 (TS-1 Catalyst, Temperature = 353- 393 K,
 % Catalyst Loading = 1.5, H_2O_2 /n-Hexane Mole Ratio = 0.2)

4.2.3 Effect of Catalyst Loading on Oxidation of *n*-Hexane at Optimal Conditions:

Figure 4.5 shows the results of experiment carried out with different % catalyst loadings. A general trend of increasing conversion and yield with increase in % catalyst loading was observed. There was no substantial increase in conversion of *n*-hexane as well as the yield after a catalyst loading of 2.33 %. The hexanol/hexanone ratio was more influenced by an increase in the catalyst amount. Since only Ti species are active centres for the reaction, an increase in Ti content leads to a more rapid conversion of *n*-hexane. But after 8 hours due to the unavailability of hydrogen peroxide, no further conversion takes place.

4.2.4 Effect of H_2O_2 /*n*-Hexane Mole Ratio on Oxidation of *n*-Hexane at Optimal Conditions:

Figure 4.6 shows the effect of hydrogen peroxide/*n*-hexane mole ratio on oxidation of *n*-hexane. While maintaining the concentration of *n*-hexane constant, experiments were carried out at different hydrogen peroxide/*n*-hexane mole ratios. Conversion increased with increasing hydrogen peroxide content, but the product yield decreased slightly due to the formation of secondary products like 1 and 2-hexanones. The hydrogen peroxide utilization was also lower due to the decomposition of it. The alcohol/ketone ratio was found to increase with decreasing hydrogen peroxide content.

4.2.5 Effect of Titanium Content in TS - 1 on the Oxidation of *n*-Hexane at Optimal Conditions and Comparison With TiZSM-5 and ZSM-5:

Three TS - 1 samples containing different Ti contents were examined for catalytic performance under identical conditions. The results are shown in Fig.4.7.

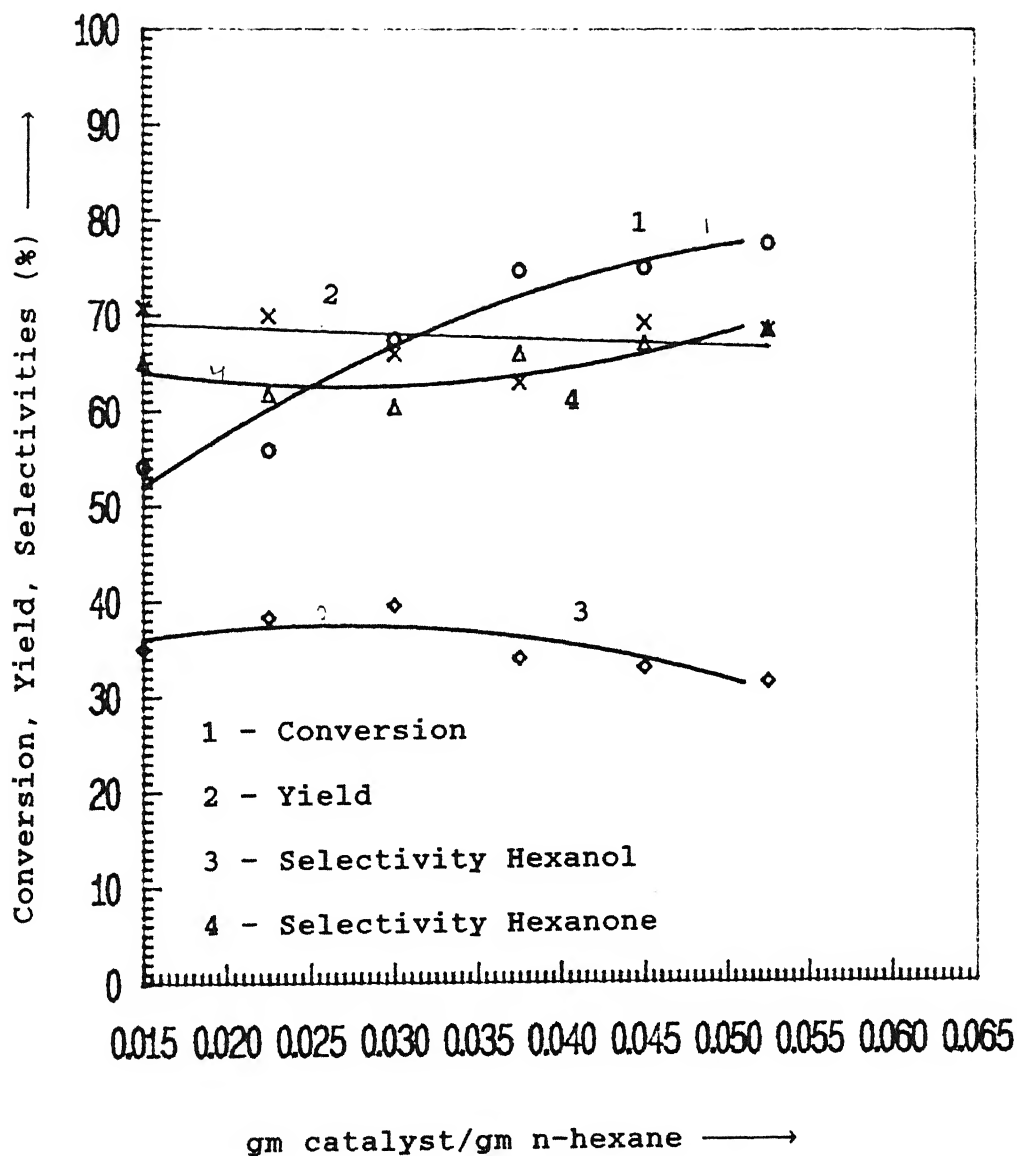


Fig 4.5 Effect of % Catalyst Loading on Conversion of n-Hexane.
Yield of Hexanol + Hexanone, Selectivities of Hexanol and Hexanone (Time = 8.48 hours, Temperature = 377 K, H_2O_2 /n-hexane mole ratio = 1.4)

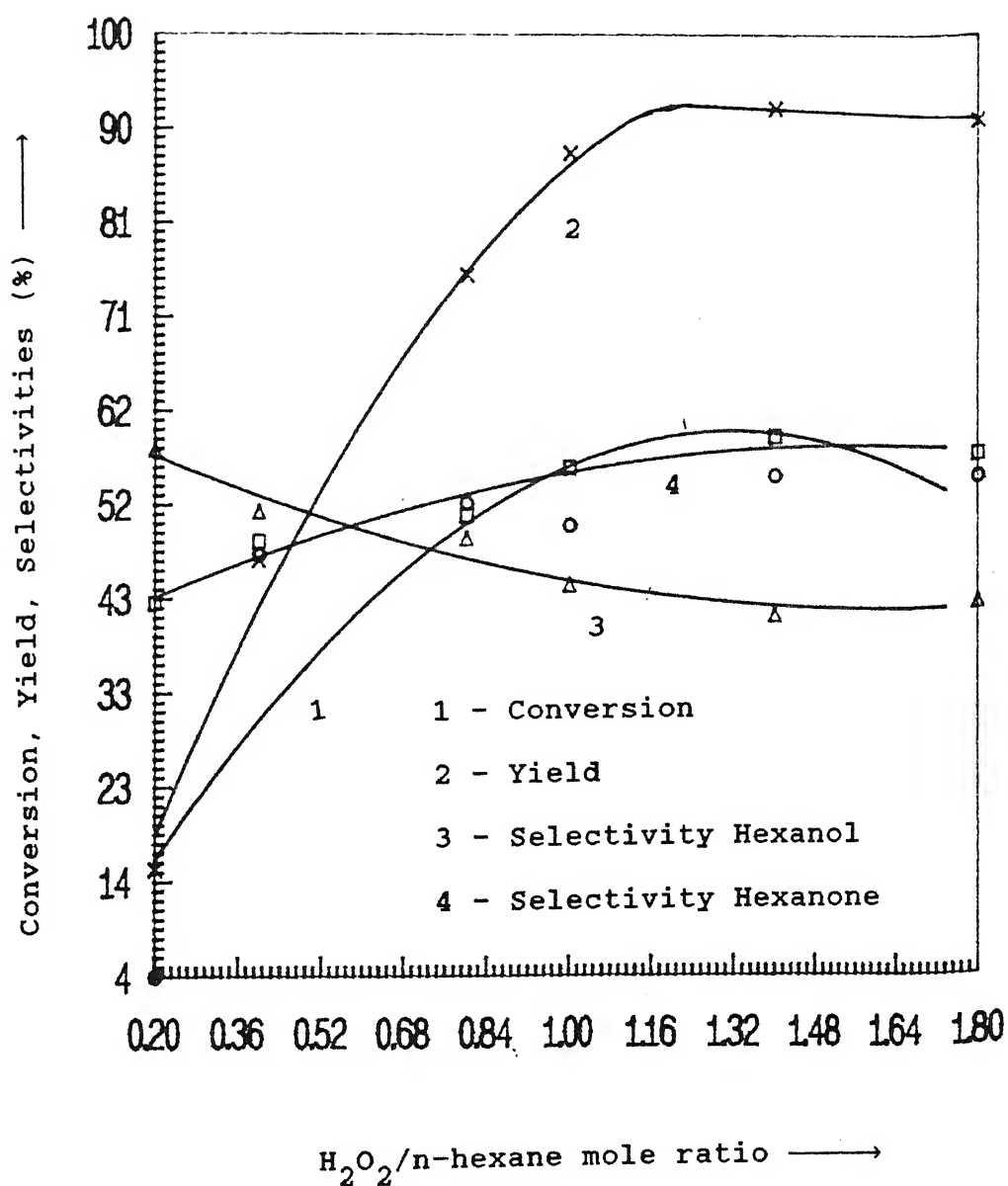


Fig 4.6 Effect of $H_2O_2/n\text{-Hexane}$ Mole Ratio on Conversion of n-Hexane, Yield of Hexanol + Hexanone, Selectivities of Hexanol and Hexanone (Time = 8.48 hours, Temperature = 377 K % Catalyst Loading = 2.33)

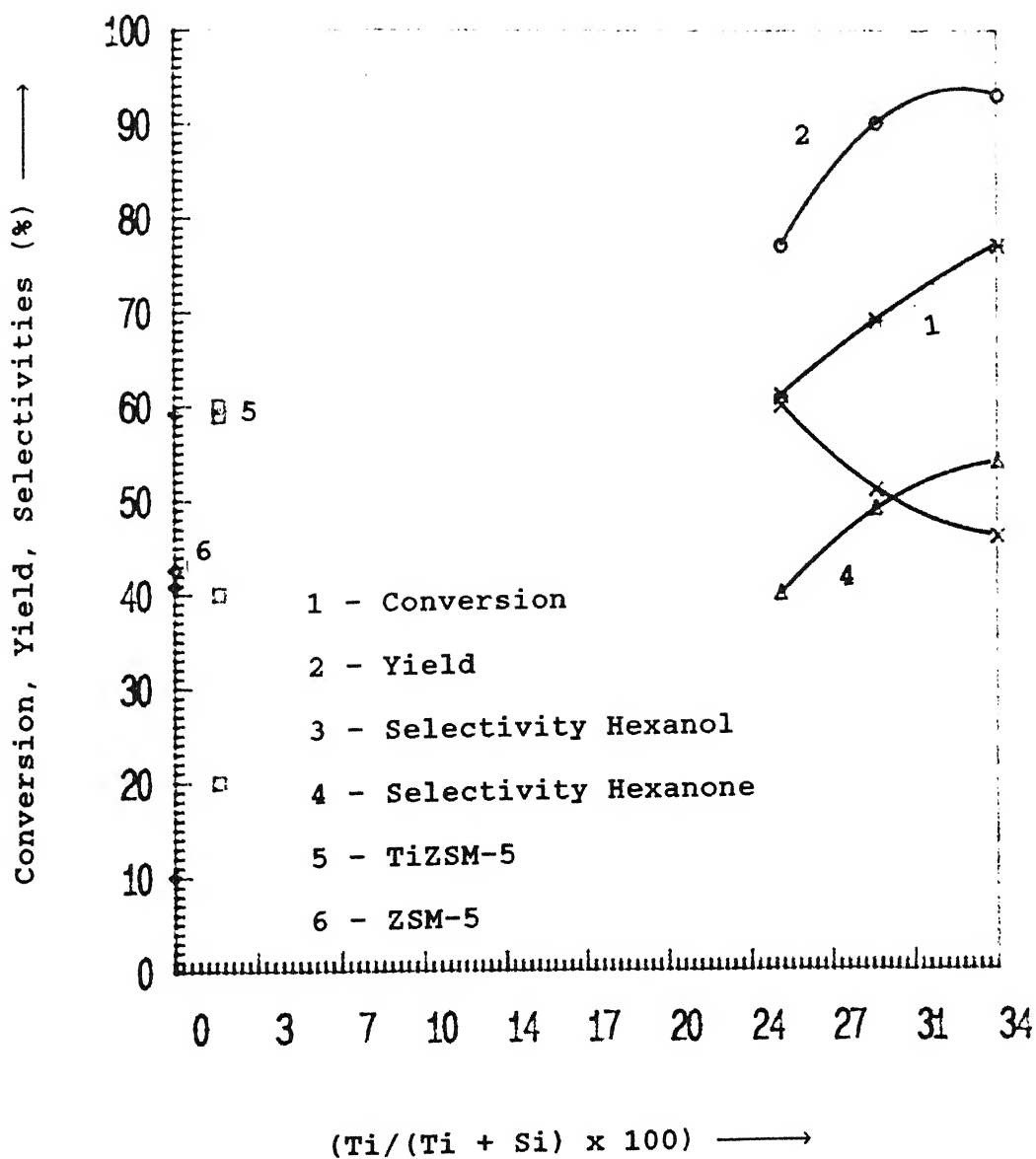


Fig 4.7 Effect of Ti Content in TS-1 Catalyst on Conversion of n-Hexane, Yield of Hexanol +Hexanone, Selectivities of Hexanol and Heanone (Time = 8 hours, Temperature = 377 K % Catalyst Loading = 2.33, H_2O_2 /n-Hexane Mole Ratio = 1.4)

The results obtained with $TiZSM - 5$ and $ZSM - 5$ were also included in the figure for comparison with $TS - 1$ catalyst. It was noticed that alcohol/ketone ratio was affected by a change in Ti content. The decrease in hexanol/hexanone ratio with increasing Ti content suggested that Ti^{4+} ions present in the catalyst catalyzed the oxidation of hexanol to hexanone.

4.3 Optimum Values of Reaction Variables

The design of experiments and response surface methodology were employed to calculate the conditions for the maximum yield of hexanol + hexanone. The coded values of the four variables calculated according to the equation 3.47 are given in Table 4.3

2^4 factorial design around the base levels were employed in the present study. Experiments were carried out in a randomized manner to avoid bias. The values of all the responses (conversion, yield and selectivities) for the first move of experiments as the design trial numbers 1 to 16 are given in Table 4.4. Design trial number 7 was repeated thrice so as to obtain the estimate of pure error.

4.3.1 Model Fitting:

The following first order model as shown in equation (3.48) has been fitted to the experimental data

$$\hat{Y} = \hat{b}_0 + \hat{b}_1x_1 + \hat{b}_2x_2 + \hat{b}_3x_3 + \hat{b}_4x_4 \quad (3.48)$$

where $\hat{b}_0, \hat{b}_1, \hat{b}_2$, and \hat{b}_3 are the best fitted values of coefficients. x_i is the i -th variable of its coded form and \hat{Y} is the predicted value of the response.

Table 4.3 First Order Response Surface Strategy: Levels of Factors

| Factor | Code | Base level | Lower level | Higher level |
|--------------------------------|-------|------------|-------------|--------------|
| Reaction Temperature (°K) | x_1 | 373 | 253 | 393 |
| Reaction time (hours) | x_2 | 8 | 4 | 12 |
| % Catalyst loading | x_3 | 2.25 | 1.5 | 3 |
| H_2O_2/n – hexane mole ratio | x_4 | 0.6 | 0.2 | 1.0 |

Table 4.4 The 2^4 First Order Design Matrix and Values of Responses

| Design Trial No. | Randomised Sequence | Factor levels in coded form | | | | | Values of Responses | | |
|------------------|---------------------|-----------------------------|-------|-------|-------|-------|---------------------|---------|---------------|
| | | x_0 | x_1 | x_2 | x_3 | x_4 | % Conversion | % Yield | % Selectivity |
| 1 | 1 | +1 | -1 | -1 | -1 | -1 | 16.1 | 20.10 | 58.10 |
| 2 | 11 | +1 | +1 | -1 | +1 | +1 | 51.1 | 76.50 | 51.40 |
| 3 | 8 | +1 | -1 | +1 | +1 | -1 | 45.7 | 32.60 | 79.90 |
| 4 | 4 | +1 | -1 | +1 | -1 | -1 | 39.9 | 30.20 | 74.60 |
| 5 | 6 | +1 | -1 | +1 | -1 | +1 | 48.7 | 75.30 | 64.50 |
| 6 | 9 | +1 | +1 | -1 | +1 | -1 | 63.0 | 40.10 | 79.70 |
| 7 | 13 | +1 | +1 | +1 | +1 | -1 | 59.8 | 38.70 | 67.20 |
| 8 | 15 | +1 | +1 | +1 | -1 | -1 | 65.8 | 41.10 | 71.00 |
| 9 | 2 | +1 | -1 | -1 | -1 | +1 | 37.2 | 70.30 | 72.70 |
| 10 | 12 | +1 | +1 | +1 | -1 | +1 | 39.3 | 71.30 | 65.70 |
| 11 | 5 | +1 | -1 | -1 | +1 | +1 | 54.1 | 78.30 | 19.40 |
| 12 | 16 | +1 | +1 | +1 | +1 | +1 | 22.1 | 64.10 | 57.90 |
| 13 | 3 | +1 | -1 | -1 | +1 | -1 | 19.7 | 21.70 | 66.70 |
| 14 | 10 | +1 | -1 | +1 | +1 | +1 | 17.5 | 62.00 | 61.40 |
| 15 | 7 | +1 | +1 | -1 | -1 | +1 | 26.7 | 66.10 | 53.20 |
| 16 | 14 | +1 | +1 | -1 | -1 | -1 | 22.7 | 23.00 | 52.70 |
| Repeat Trials | | | | | | | | | |
| 17 | 18 | +1 | +1 | -1 | -1 | +1 | 21.9 | 64.00 | 59.90 |
| 18 | 17 | +1 | +1 | -1 | -1 | +1 | 20.9 | 63.80 | 41.60 |

The coefficients can be estimated by the least square technique as in equation (3.49)

as

$$\hat{\underline{b}} = (\underline{X}^T \underline{X})^{-1} \underline{X}^T \underline{Y} \quad (3.49)$$

where \underline{X} is the design matrix, \underline{X}^T is the transpose of the design matrix, \underline{Y} is the vector of responses and $\hat{\underline{b}}$ is the vector of coefficients. The fitted first order models for the conversion of *n*-hexane, yield of (hexanol + hexanone) and selectivity of hexanol are given below by equations 4.1, 4.2 and 4.3

$$\hat{Y}_C = 39.3325 + 4.976x_1 + 3.001x_2 + 2.28x_3 + 2.2575x_4 \quad (4.1)$$

$$\hat{Y}_Y = 50.7025 + 1.8975x_1 + 1.9125x_2 + 1.035x_3 + 19.785x_4 \quad (4.2)$$

$$\hat{Y}_S = 62.246 + 0.09625x_1 + 5.5125x_2 - 1.80625x_3 - 6.483x_4 \quad (4.3)$$

where \hat{Y}_C , \hat{Y}_Y and \hat{Y}_S represents the predicted values of % conversion of *n*-hexane, % yield of (hexanol + hexanone) and % selectivity of hexanol. The lack-of fit \bar{F} test for the above models are shown in Tables 4.5 through 4.7 respectively.

4.3.2 Calculation of The Path of Steepest Ascent and Conduct of Experiments Along this Path:

The direction of steepest ascent was described as in equation (3.50) as

$$\nabla \Phi = \frac{\delta \phi}{\delta x} \bar{u}_1 + \frac{\delta \phi}{\delta x} \bar{u}_2 + \dots + \frac{\delta \phi}{\delta x} \bar{u}_k \quad k = 1, 2, \dots, n \quad (3.50)$$

Table 4.5. First Order Response Surface Strategy: Test for the Adequacy of the Model for % conversion of n-Hexane

$$\text{Model : } \hat{Y}_C = 39.3325 + 4.4762x_1 + 3.01125x_2 + 2.28x_3 - 2.2575x_4$$

ANOVA

| Source | Sum of Squares | Degrees of Freedom | Mean Square |
|-------------------|----------------|--------------------|-------------|
| Due to Regression | 4880 | 4 | |
| Residual | 4140 | 13 | |
| Pure Error | 18.7 | 2 | 9.33 |
| Lack-of-Fit | 4120 | 11 | 374.6 |
| Total | 9000 | 17 | |

$$F_{\text{cal}} = 374.6/9.33 = 40.1$$

$$F_{0.01(11,2)} = 99.42$$

$$F_{\text{cal}} < F_{0.01(11,2)}$$

Therefore, the model is adequate

Table 4.6. First Order Response Surface Strategy: Test for the Adequacy of the Model for % Yield of (Hexanol + Hexanone)

$$\text{Model : } \hat{Y}_Y = 50.7025 + 1.8975x_1 + 1.191x_2 + 1.035x_3 + 19.785x_4$$

ANOVA

| Source | Sum of Squares | Degrees of Freedom | Mean Square |
|-------------------|----------------|--------------------|-------------|
| Due to Regression | 7341 | 4 | |
| Residual | 749 | 13 | |
| Pure Error | 19.2 | 2 | 9.61 |
| Lack-of-Fit | 730 | 11 | 66.34 |
| Total | 8071 | 17 | |

$$F_{\text{cal}} = 66.34/9.61 = 6.9$$

$$F_{0.01(11,2)} = 99.42$$

$$F_{\text{cal}} < F_{0.01(11,2)}$$

Therefore, the model is adequate.

Table 4.7. First Order Response Surface Strategy: Test for the Adequacy of the Model for % Selectivity of Hexanol

$$\text{Model : } \hat{Y}_s = 62.24625 + 0.0962x_1 + 5.512x_2 - 1.8x_3 - 6.483x_4$$

ANOVA

| Source | Sum of Squares | Degrees of Freedom | Mean Square |
|-------------------|----------------|--------------------|-------------|
| Due to Regression | 3579 | 4 | |
| Residual | 2138 | 13 | |
| Pure Error | 171 | 2 | 85.5 |
| Lack-of-Fit | 1967 | 11 | 178.8 |
| Total | 5546 | 17 | |

$$F_{\text{cal}} = 178.8/85.5 = 2.08$$

$$F_{0.01(11,2)} = 99.42$$

$$F_{\text{cal}} < F_{0.01(11,2)}$$

Therefore, the model is adequate.

where ϕ is the function describing the response surface,

$\nabla\phi$ is the gradient of response function,

$\frac{\partial\phi}{\partial x}$ is the partial derivative of function with respect to the i -th factor,

and $\bar{u}_1, \bar{u}_2, \dots, \bar{u}_k$ are unit vectors in the direction of coordinate axes. By changing the corresponding variables x_1 (*Temperature*), x_2 (*Time*), x_3 (% Catalyst loading) and x_4 (hydrogen peroxide/*n*-hexane mole ratio) in proportion to the values of their corresponding coefficients, the movement along the steepest path is realised. From the coefficients of the fitted model for yield (Equation (4.2)), it is easy to compute these factor level combinations which predict an increase in the yield of (hexanol + hexanone). The calculation of this path is shown in Table 4.8. The details of these calculations are described below.

First two rows of the table indicate the values of the base levels and variation intervals of different factors. In the third row the regression coefficients of the model are given. The coefficients represent the gradients of the yield in their respective directions. The fourth row was obtained by multiplying the unit of each factor with its coefficient so as to change the factor level in proportion to its slope (i.e. its regression coefficients). In the fifth row step changes in the factors x_1, x_2 and x_3 were calculated corresponding to a change of 0.2 in the direction of x_4 . The choice of step size is a matter of experimental convenience. The fifth row was then added to the original base levels in the first row, element by element, to get the elements of the first trial point in the path of steepest ascent. The second trial point in the path was obtained by adding elements of first trial point to the elements of the fifth row.

Table 4.8 First Order Response Surface Strategy: Calculations of the Path of Steepest Ascent

| | Factor | | | |
|--|--------|--------|--------|--------|
| | X_1 | X_2 | X_3 | X_4 |
| Base Level : | 373 | 8 | 2.25 | 0.6 |
| Unit : | 20 | 4 | 0.75 | 0.4 |
| Estimated Slope (b) : | 1.8975 | 1.1912 | 1.035 | 19.785 |
| Unit ($x * b$) | 37.95 | 4.765 | 0.7762 | 7.914 |
| Change in Level Per : 0.2 change in X_4 | 1 | 0.12 | 0.02 | 0.2 |

Path of Steepest Ascent as Represented by a Series of Trial Points

| Trial Point | X_1 | X_2 | X_3 | X_4 |
|-------------|-------|-------|-------|-------|
| 1 | 374 | 8.12 | 2.27 | 0.8 |
| 2 | 375 | 8.24 | 2.29 | 1.0 |
| 3 | 376 | 8.36 | 2.31 | 1.2 |
| 4 | 377 | 8.48 | 2.33 | 1.4 |

Additional experiments were then performed according to trial points 1 through 4. The experimental results and values predicted by the first order model (Equation (4.2)) are given in Table 4.9. The predicted yields were calculated by using equation (4.2) after the factors were coded using equation (3.47). It was observed from Table 4.9 that the experimental yield values increase to a maximum value of 93.25 at settings in x_1, x_2, x_3 and x_4 of 104°C , 8.48 hours, catalyst loading of 2.33% and $\text{H}_2\text{O}_2/n\text{-hexane}$ mole ratio of 1.4. Table 4.10 presents optimum values of factor levels and the yield of (hexanol + hexanone).

4.4 Characterization Studies

4.4.1 X-Ray Diffraction of TS – 1 Catalyst:

Powdered x-ray diffraction patterns of fresh and used catalyst were obtained using REICH-SEIFERT ISO-DEBYEFLEX 2002 diffractometer (Ni -filter, GuK_α radiation). Figure 4.8a, b and c present the x-ray diffraction patterns of ZSM-5 catalyst and fresh and regenerated TS – 1 catalysts. The XRD pattern for TS – 1 is characteristic of MFI type structure of ZSM-5. Upon calcination at 823K in air (to remove TPA^+ ions), TS – 1 retained its orthorhombic symmetry. The peak at $2\theta = 23.5^\circ$ which is characteristic of ZSM-5 further confirmed that the catalyst is of MFI type. XRD pattern of the regenerated catalyst was performed to check about phase changes occurred if any, during the reaction. The persistence of the orthorhombic symmetry even in the calcined samples of TS – 1 catalyst is indicative of the location of Ti in the zeolite framework.

Table 4.9. First Order Response Surface Strategy : Results of Experiments Along the Path of Steepest Ascent

| Trial Point | Experimental % Yield | Predicted % Yield |
|-------------|----------------------|-------------------|
| 1 | 58.9 | 60.7 |
| 2 | 74.8 | 70.8 |
| 3 | 83.5 | 80.9 |
| 4 | 93.3 | 90.0 |

Table 4.10. Optimum Values of factor Levels and the Yield of (Hexanol + Hexanone)

| Factor | Code | Coded Value | Natural Value |
|-----------------------------------|-------|-------------|---------------|
| Reaction Temp. (°K) | x_1 | 0.2 | 104 |
| Reaction Time (hours) | x_2 | 0.12 | 8.48 |
| Catalyst Loading (%) | x_3 | 0.106 | 2.33 |
| H_2O_2/n – hexane mole ratio | x_4 | 2 | 1.4 |

The estimated yield of (hexanol + hexanone) at the optimum values of factor levels is 93.3% .

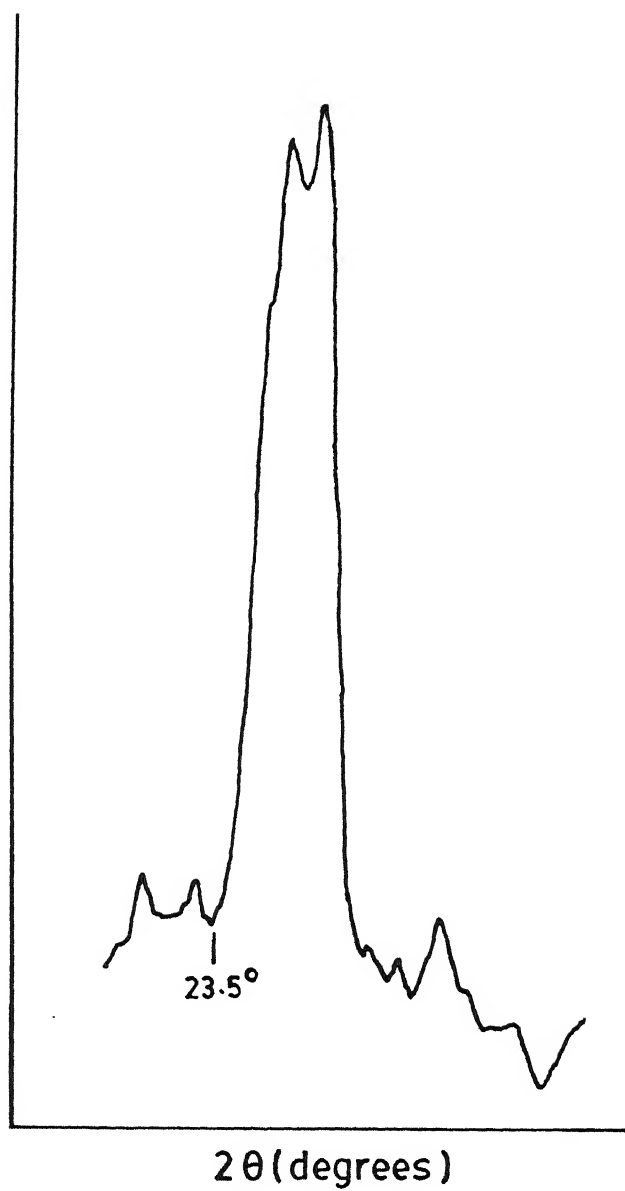


Fig 4.8a X-Ray Diffraction Pattern of ZSM-5 Catalyst

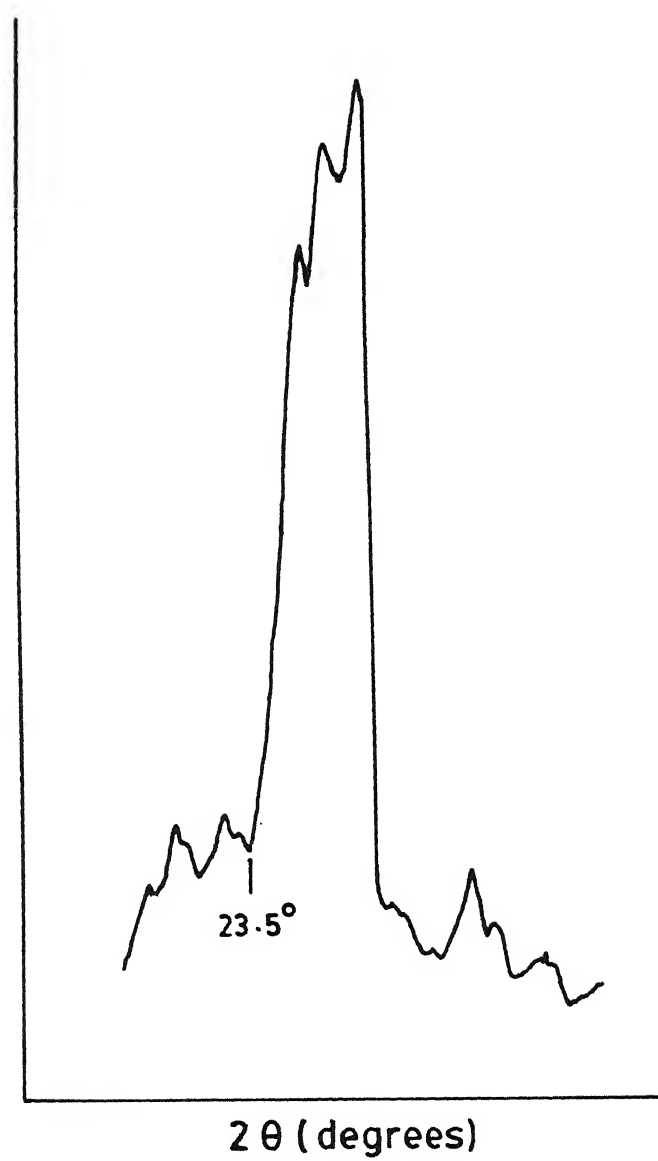


Fig 4.8b X-Ray Diffraction Pattern of Fresh TS-1 Catalyst

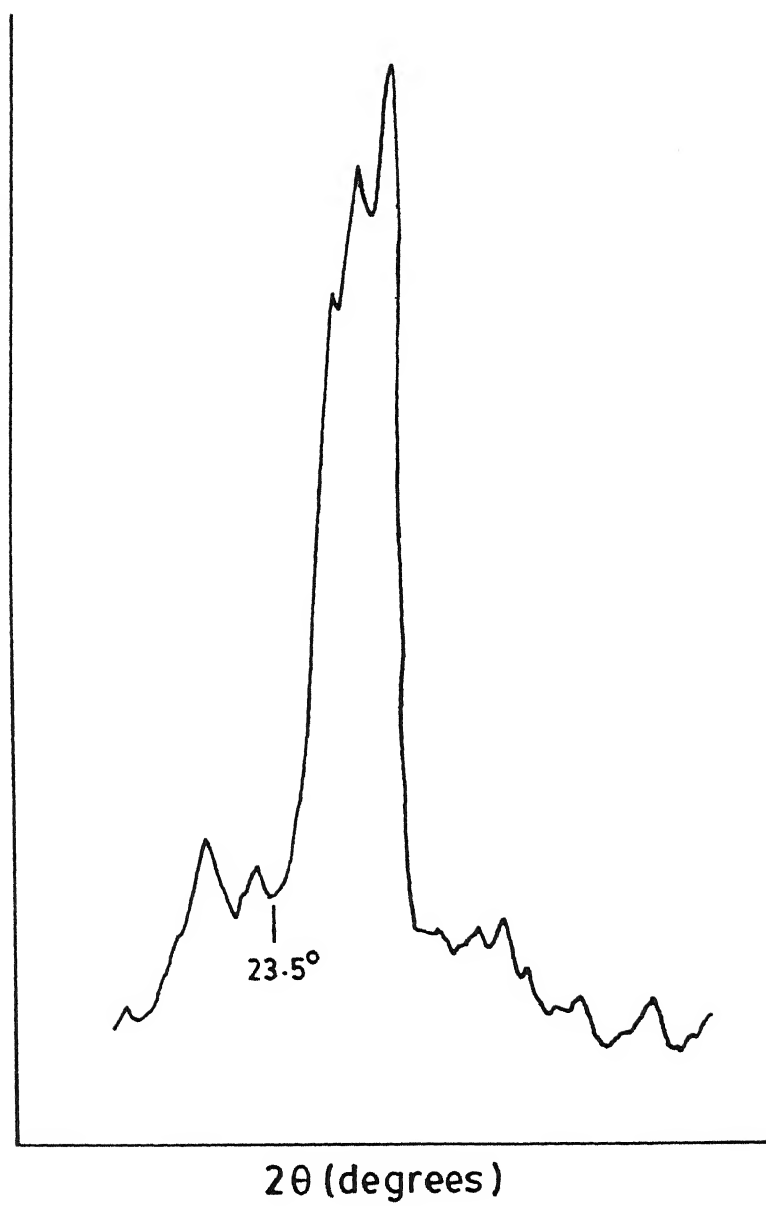


Fig 4.8c X-Ray Diffraction Pattern of Regenerated TS-1 Catalyst

(a) TiZSM - 5

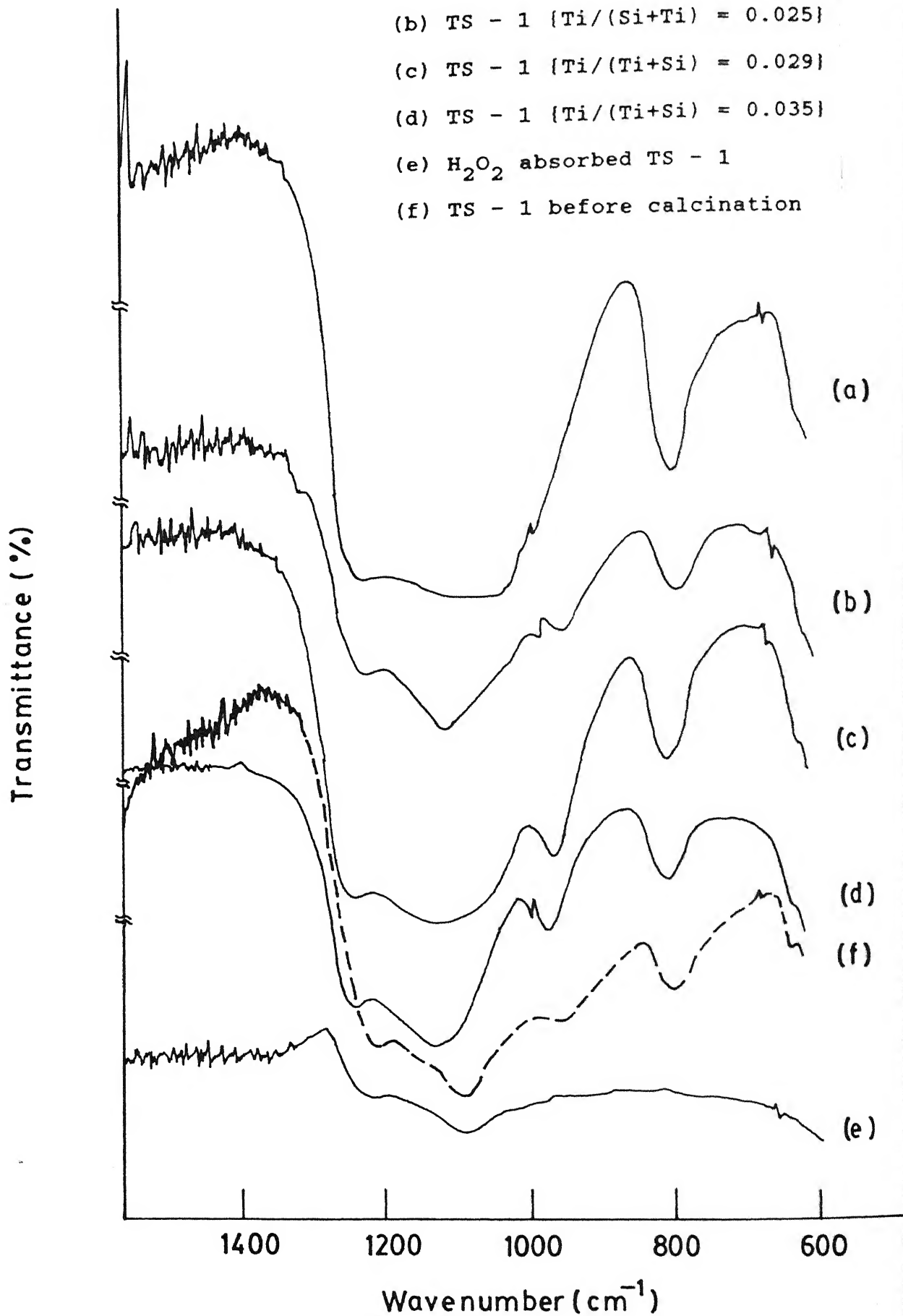
(b) TS - 1 {Ti/(Si+Ti) = 0.025}

(c) TS - 1 {Ti/(Ti+Si) = 0.029}

(d) TS - 1 {Ti/(Ti+Si) = 0.035}

(e) H₂O₂ absorbed TS - 1

(f) TS - 1 before calcination



4.4.2 Infra Red Spectroscopy:

Infra red spectroscopic measurements were carried out using a Perkin Elmer 1320 spectrometer to know whether titanium has been substituted in the catalyst or not. Figure 4.9 shows the framework *IR* spectra of different samples of *TS* - 1, with different titanium contents and, and TiZSM-5. An absorption band at 960cm^{-1} has been observed in the case of all the samples. The relative intensity of this band increased with *Ti* contents. The band at $950 - 970\text{cm}^{-1}$ has been attributed to *Ti* incorporation in zeolite framework. In the case of calcined *TS* - 1, this band has been assigned to the polarized $\text{SiO}^{\delta+} \dots \text{Ti}^{\delta+}$ bond or to a titanyl group ($\text{Ti} = \text{O}$) and is generally a proof for the incorporation of *Ti* into the zeolite framework. The intensity of the 960cm^{-1} band in calcined samples was found to be more than that before calcination. This is due to the presence of organic template in the catalyst before calcination. Figure 4.9 also shows the *IR* spectra of H_2O_2 absorbed on *TS* - 1 catalyst. The disappearance of 960cm^{-1} band indicates that peroxy sites were formed on *TS* - 1 catalyst.

4.4.3 Scanning Electron Microscopy :

Figures 4.10a, 4.10b and 4.10c and 4.10d show SEM pictures of *TS* - 1 catalyst before and after calcination, *TS* - 1 with increased titanium content and of TiZSM-5 taken by using JOEL, JSM-840A scanning electron microscope to measure the particle size. The sample consists of crystals of uniform size (100nm) and shape (cuboid). The small size of *TS* - 1 when compared to other catalysts is due to the crystallization of *TS* - 1 at a faster rate. The size of the particles increased with increase in *Ti* content in the catalyst. The size observed for *TS* - 1 with Si/*Ti* mole ratio of 28 is $10\mu\text{m}$. As seen in Fig. 4.10a, the presence of organic template before calcination, the particles are clustered. The particles with size of 100nm are cubic in shape whereas the particles with size of $10\mu\text{m}$ are more spherical with irregular surface which is due to the addition of titanium.

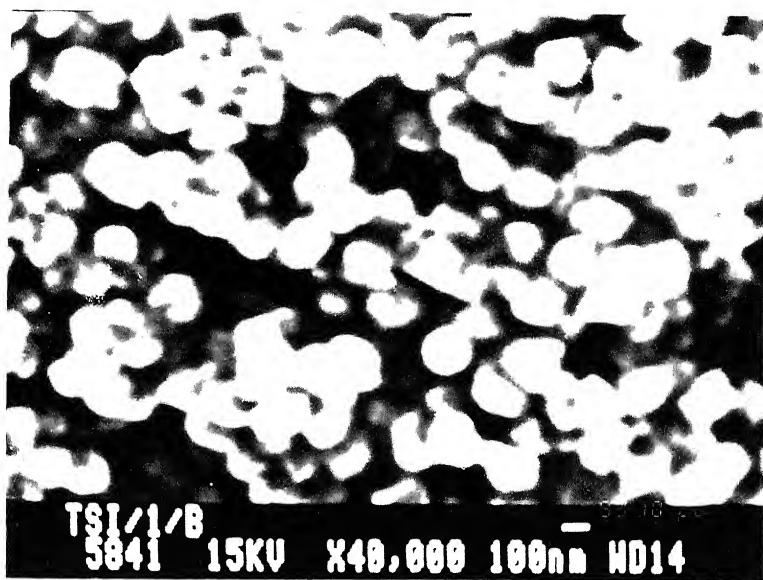


Fig 4.10a SEM Micrograph of TS-1 Catalyst Before Calcination

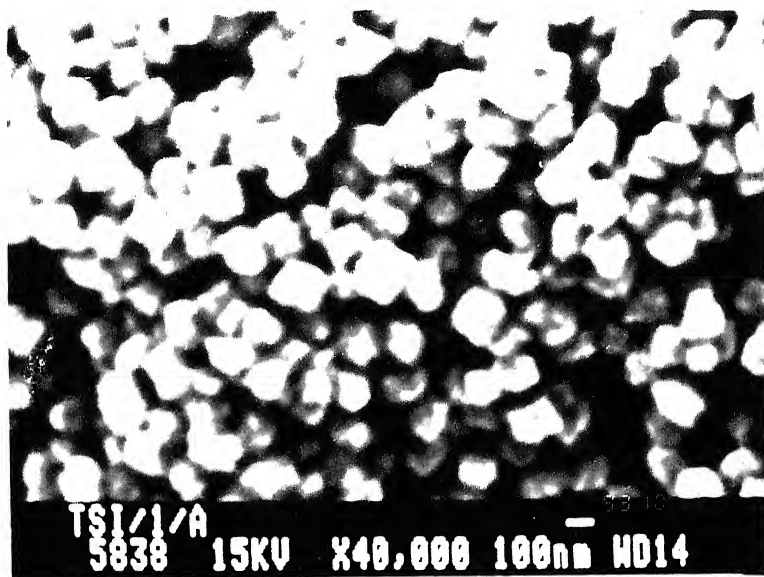


Fig 4.10b SEM Micrograph of TS-1 Catalyst After Calcination
(Ti/(Ti + Si) =0.029)

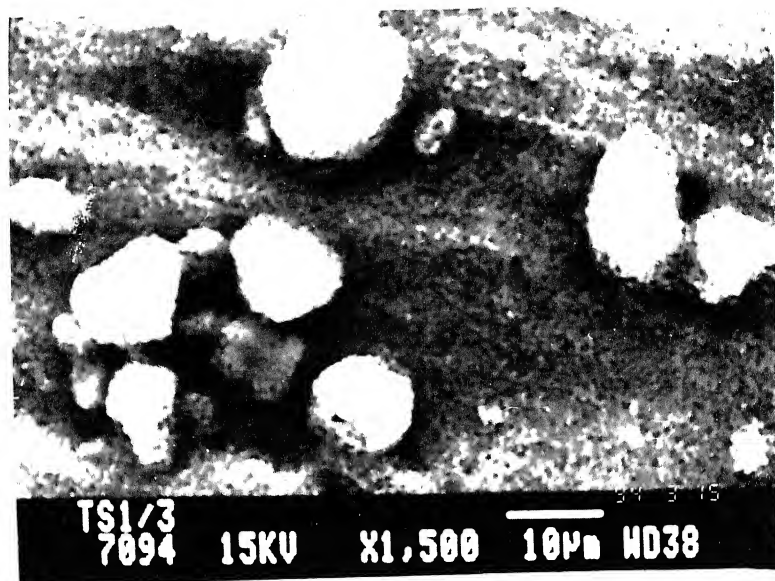


Fig 4.10c SEM Micrograph of TS-1 with $\text{Ti}/(\text{Ti} + \text{Si}) = 0.035$

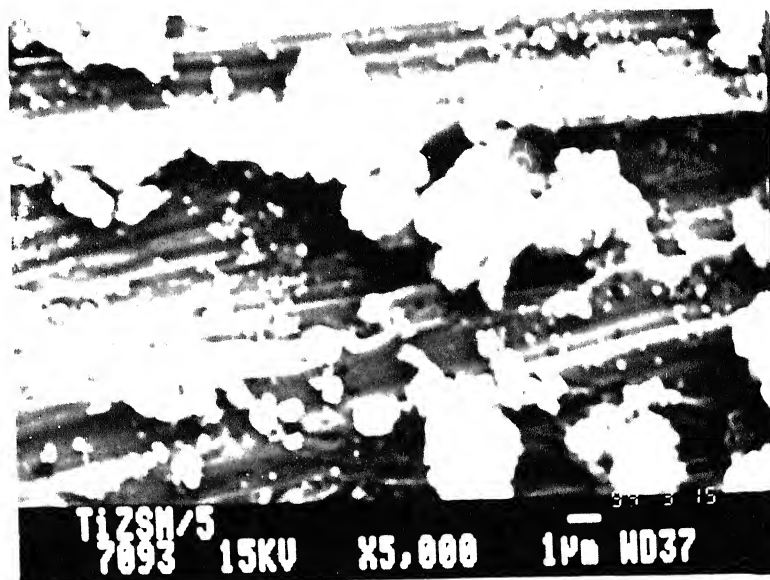


Fig 4.10d SEM Micrograph of TiZSM-5

BET surface area measurements showed a large surface area of $TS - 1$ catalyst. The surface area measured was $514m^2/\text{gram}$ of catalyst.

4.5 Kinetic Modelling

Kinetic data of the oxidation of *n*-hexane with hydrogen peroxide, were obtained at different temperatures with varying reaction times, a constant catalyst loading of 1.5% and a constant H_2O_2/n -hexane mole ratio of 0.2 on $TS - 1$ catalyst. Kinetic data are given in Appendix A. Typical kinetic data obtained at a reaction temperature of $383K$ are given in Table 4.11.

4.5.1 Homogeneous Model:

This model was already presented in chapter 3. The following equations were considered to obtain the reaction rate constants k_1 and k_2 .

$$(-r_A) = k_1 C_A C_B \quad (3.8)$$

$$(r_C) = k_1 C_A C_B - k_2 C_B C_C \quad (3.10)$$

The rate constants in the above equations were estimated using linear regression technique (Gupta, S.K., 1992) by minimizing the objective function as shown in equation (3.16).

The rate constants k_1 and k_2 evaluated at different temperatures are reported in Table 4.12 for $TS - 1$ catalyst. The apparent activation energies and pre-exponential factors were calculated by plotting the data as shown in Fig. 4.11. The logarithm of reaction rate constants k_1 and k_2 were plotted against the reciprocal of reaction temperature in the form of Arrhenius plot as shown in Fig. 4.11.

Table 4.11 Typical Experimental Kinetic Data on $TS-1$ catalyst

H_2O_2/n -hexane mole ratio = 0.2

% Catalyst loading (gm catalyst/ gmn -hexane $\times 100$) = 1.5

Reaction Temperature = $383K$

| Time hours | C_A gmol/cc $\times 10^3$ | C_B gmol/cc $\times 10^3$ | C_C gmol/cc $\times 10^3$ | C_D gmol/cc $\times 10^3$ | Rate gmol/gcat-sec $\times 10^{11}$ |
|---------------|-----------------------------------|-----------------------------------|-----------------------------------|-----------------------------------|---|
| 3 | 4.98 | 3.61 | 1.53 | 1.53 | 9.77 |
| 4 | 4.76 | 3.39 | 1.75 | 1.75 | 8.40 |
| 5 | 4.50 | 3.13 | 2.01 | 2.01 | 7.22 |
| 6 | 4.28 | 2.92 | 2.22 | 2.23 | 6.53 |
| 7 | 3.90 | 2.53 | 2.61 | 2.61 | 5.44 |
| 8 | 3.85 | 2.48 | 2.66 | 2.66 | 4.92 |
| 9 | 3.78 | 2.42 | 2.72 | 2.72 | 4.36 |
| 10 | 3.77 | 2.41 | 2.73 | 2.73 | 3.94 |
| 11 | 3.77 | 2.40 | 2.73 | 2.74 | 3.55 |
| 12 | 3.76 | 2.39 | 2.71 | 2.75 | 3.25 |

Table 4.12 Effect of Reaction Temperature on Rate Constants Over *TS - 1* Catalyst (Homogeneous Model)

| Temperature ($^{\circ}K$) | k_1 $gmol/cc - sec$ $\times 10^6$ | k_2 $gmol/cc - sec$ $\times 10^{10}$ |
|--------------------------------|---|--|
| 353 | 8.73 | 25.5 |
| 363 | 4.80 | 21.6 |
| 373 | 3.34 | 1.23 |
| 383 | 0.54 | 1.30 |
| 393 | 0.50 | 1.15 |

| | Activation Energy | Pre-exponential Factors $\times 10^{-4}$ |
|-------|-------------------|---|
| k_1 | 90.7 | 1080 |
| k_2 | 102.3 | 10.3 |

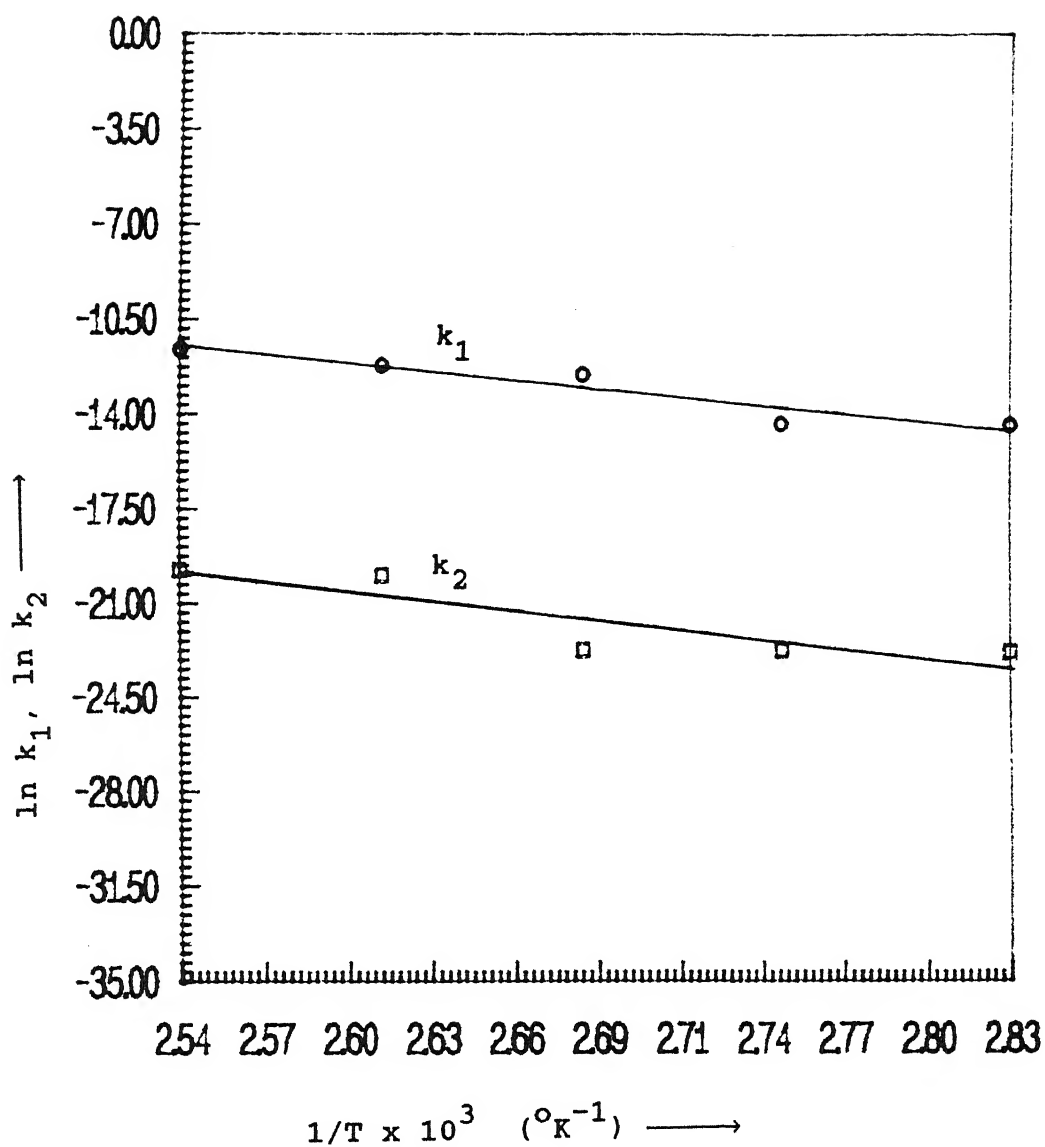


Fig 4.11 Arrhenius Plot of Reaction Rate Constants (Homogeneous Model). Curves (1) k_1 (2) k_2

4.5.2 Heterogeneous Model:

Different heterogeneous models based on LHHW approach were discussed in chapter 3. Single site and Dual site mechanisms were considered for kinetic data analysis. Different types of rate expressions based on the above two mechanisms were given in Table 3.1 for oxidation of *n*-hexane.

The reaction data can be calculated as follows:

- 1) Experimental values of *n*-hexane conversion (X_A) vs time was plotted at different reaction temperatures.
- 2) Smoothened curves were obtained by cubic fitting (best fit) from experimental data.
- 3) Slope of these curves at different times multiplied by initial concentration of *n*-hexane will give rate ($-r_A = C_{A0} \frac{dX_A}{dt}$).

Using the above rates along with concentration data given in Appendix A, various models as given in chapter 3 were tested. The following criteria was used for the discrimination among various models:

- 1) If any of the parameters are found to be negative by fitting the experimental data in the model, then the model is discarded.
- 2) If the parameters are all positive but there is high irregularity in their behaviour (e.g. adsorption and desorption constants should decrease and surface reaction constant should increase with increase in reaction temperature), the model is rejected (Froment, Bischoff, 1990).

- 3) In a particular model, the rate corresponding to the reaction controlling step should have the lowest value.
- 4) If more than one model satisfy the above criteria then the model having minimum error (i.e. minimum RSS) is accepted.

The parameters were evaluated for various models and are given in Table 4.13 using non-linear regression method based on Rosen Brock optimization technique (Kuester and Mize). Initial guesses were obtained by linear regression method.

After testing the above two models, surface reaction in single site mechanism satisfied all the above criteria for oxidation of *n*-hexane. The plausible model which satisfied the above criteria is given below.

$$r_{sr} = \frac{k_{sr1}C_A C_B + k_{sr2}C_B C_C}{\frac{1}{K_A} + C_B + \frac{K_{D1}}{K_A C_C} + \frac{K_{D2}}{K_A C_D}}$$

where K_{sr1} and k_{sr2} are surface reaction constants, gmol/gcat-sec

K_A, K_{D1}, K_{D2} are adsorption and desorption constants, cc/gmol-gcat

The parameters are given in Table 4.13

The effect of reaction temperature on all parameters are plotted in the form of Arrhenius plot as shown in Fig. 4.12 and Fig. 4.13. The apparent activation energy of reaction, pre-exponential factors, heat of adsorption and desorption were also calculated and are given in Table 4.14.

Table 4.13 Effect of Reaction Temperature on Reaction Parameters on *TS-1* Catalyst

| Temperature ($^{\circ}K$) | k_{sr1} $\frac{gmol}{gcat - sec}$ $\times 10^{13}$ | k_{sr2} $\frac{gmol}{gcat - sec}$ $\times 10^8$ | K_A $\frac{cc}{gmol-gcat}$ $\times 10^{-17}$ | K_{D1} $\frac{cc}{gmol-gcat}$ $\times 10^{-4}$ | K_{D2} $\frac{cc}{gmol-gcat}$ |
|--------------------------------|--|---|--|--|------------------------------------|
| 353 | 4.86 | 2.87 | 5.52 | 2.15 | 536 |
| 363 | 21.3 | 5.07 | 1.43 | 1.44 | 412 |
| 373 | 62.1 | 10.03 | 0.41 | 0.99 | 321 |
| 383 | 200 | 46.21 | 0.13 | 0.7 | 253 |
| 393 | 600 | 113 | 0.04 | 0.5 | 202 |

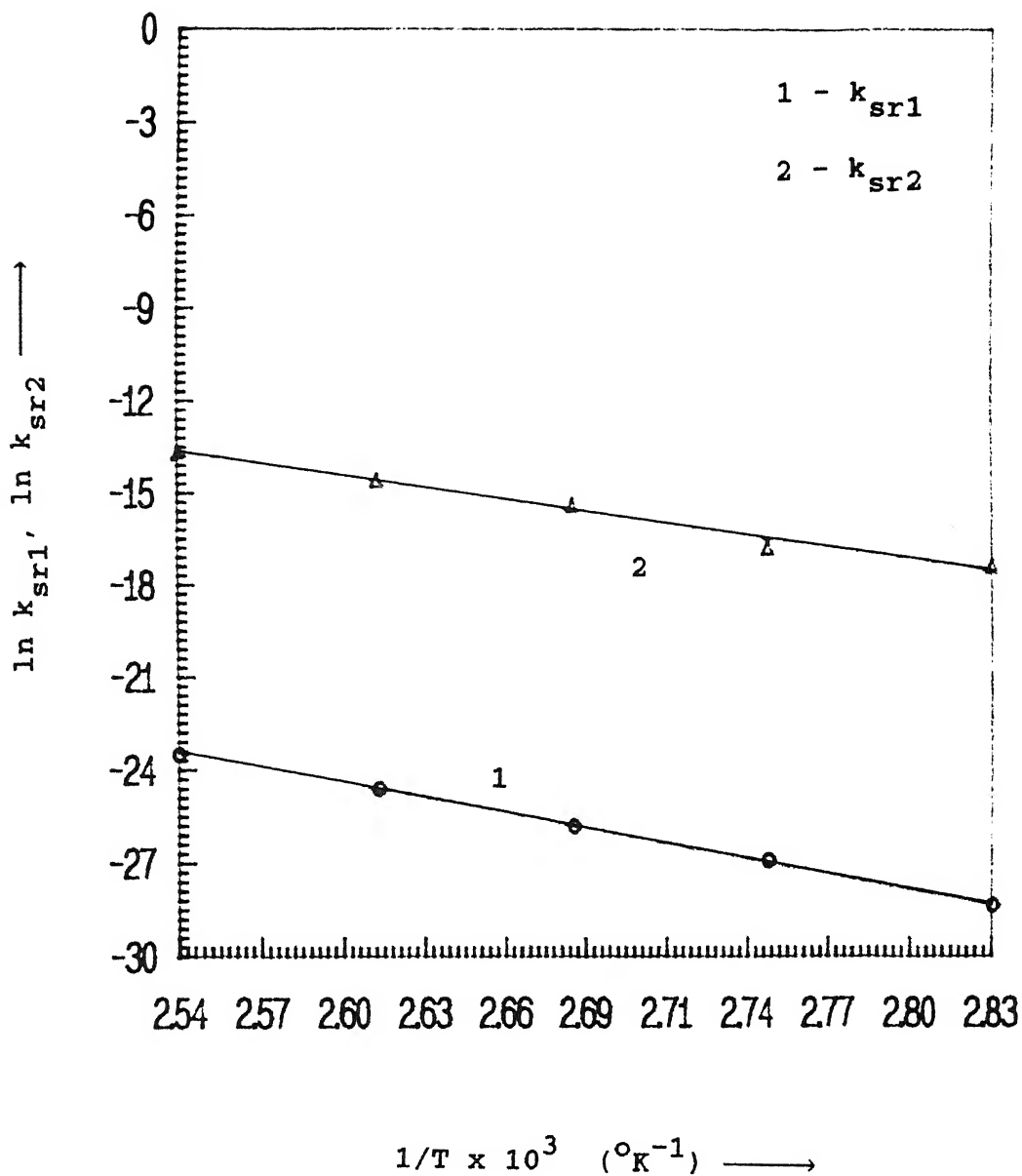


Fig 4.12 Arrhenius Plot of Reaction Rate Constants (Heterogeneous Model). Curves (1) k_{sr1} (2) k_{sr2}

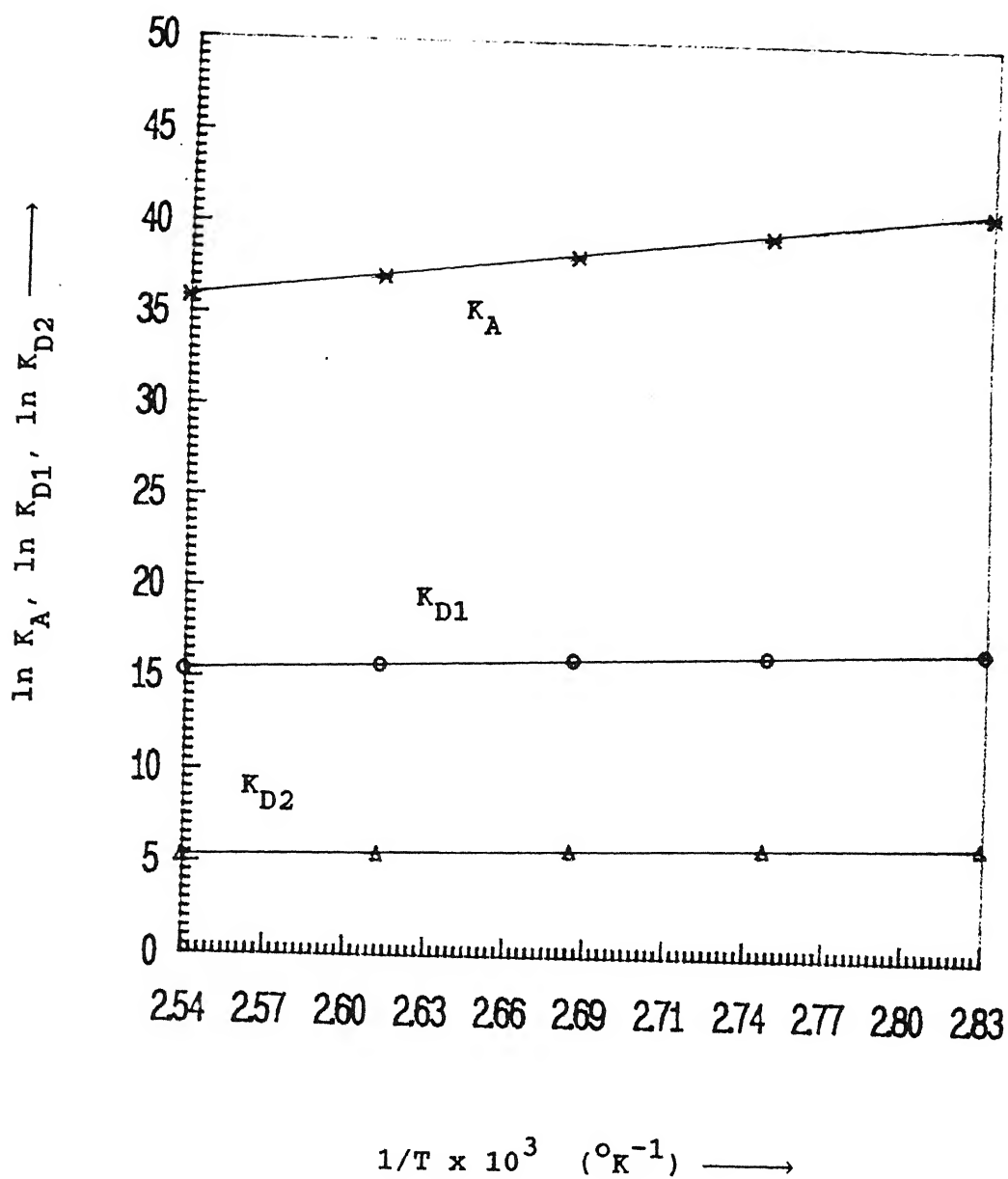


Fig 4.13 Arrhenius Plot of Reaction Rate Constants (Heterogeneous Model). Curves (1) K_A (2) K_{D1} (3) K_{D2}

Table 4.14 Values of Activation Energy, Pre-exponential Factors, Heats of Adsorption and Desorption (Heterogeneous Model)

| | |
|---|-------------------|
| Activation Energy E_{sr1} , $KJ/gmol$ | 140 |
| Activation Energy E_{sr2} , $KJ/gmol$ | 110.6 |
| Heat of Adsorption H_A , $KJ/gmol$ | -142.2 |
| Heat of Desorption H_{D1} , $KJ/gmol$ | -42.8 |
| Heat of Desorption H_{D2} , $KJ/gmol$ | -28.9 |
| Pre-exponential Factor, k_{sr10} | 2.4×10^8 |
| Pre-exponential Factor, k_{sr20} | 5.4×10^8 |

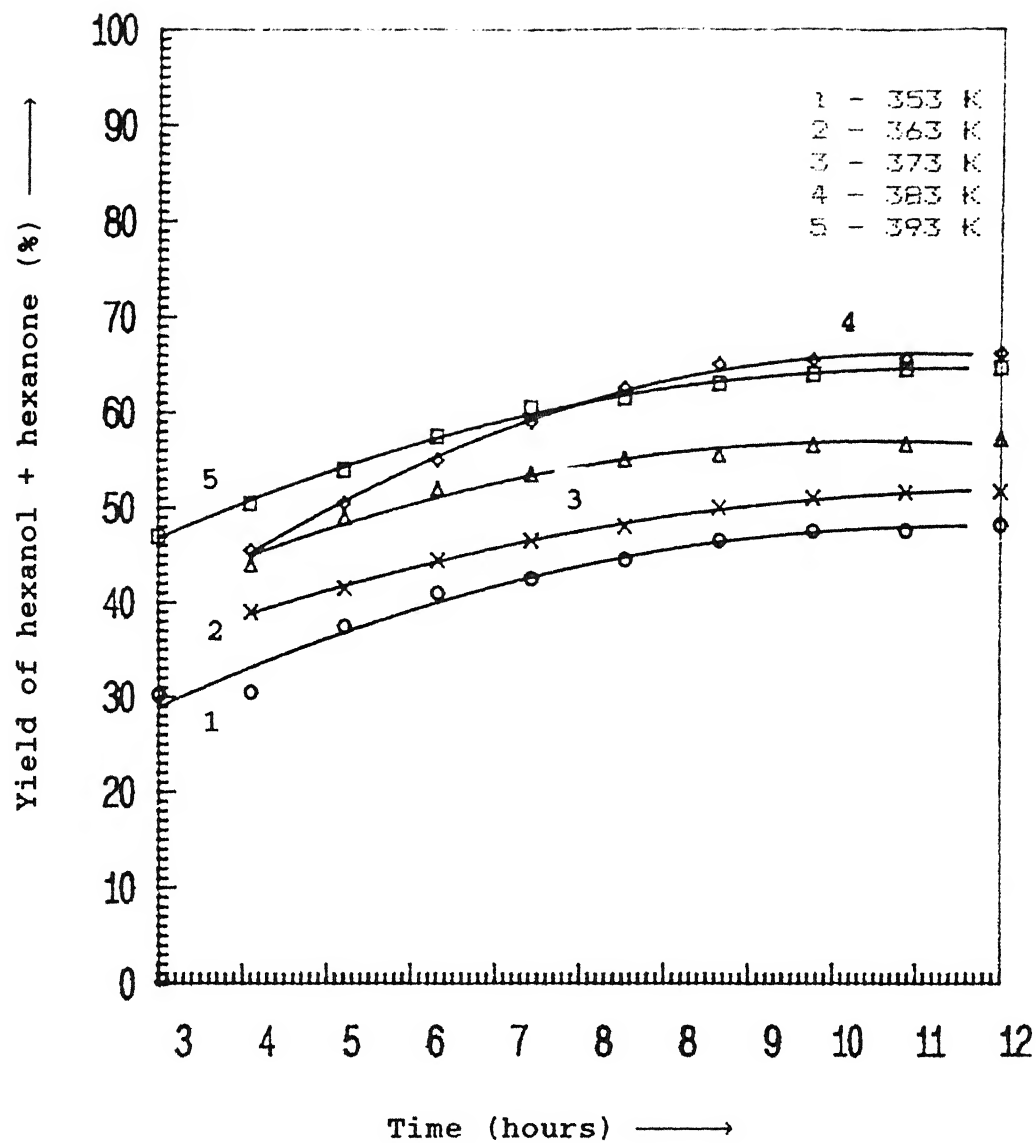


Fig 4.14 % Yield of Hexanol + Hexanone versus Time

(Temperature = 353 - 393 K, % Catalyst Loading = 1.5,
 $\text{H}_2\text{O}_2/\text{n-Hexane}$ Mole Ratio = 0.2)

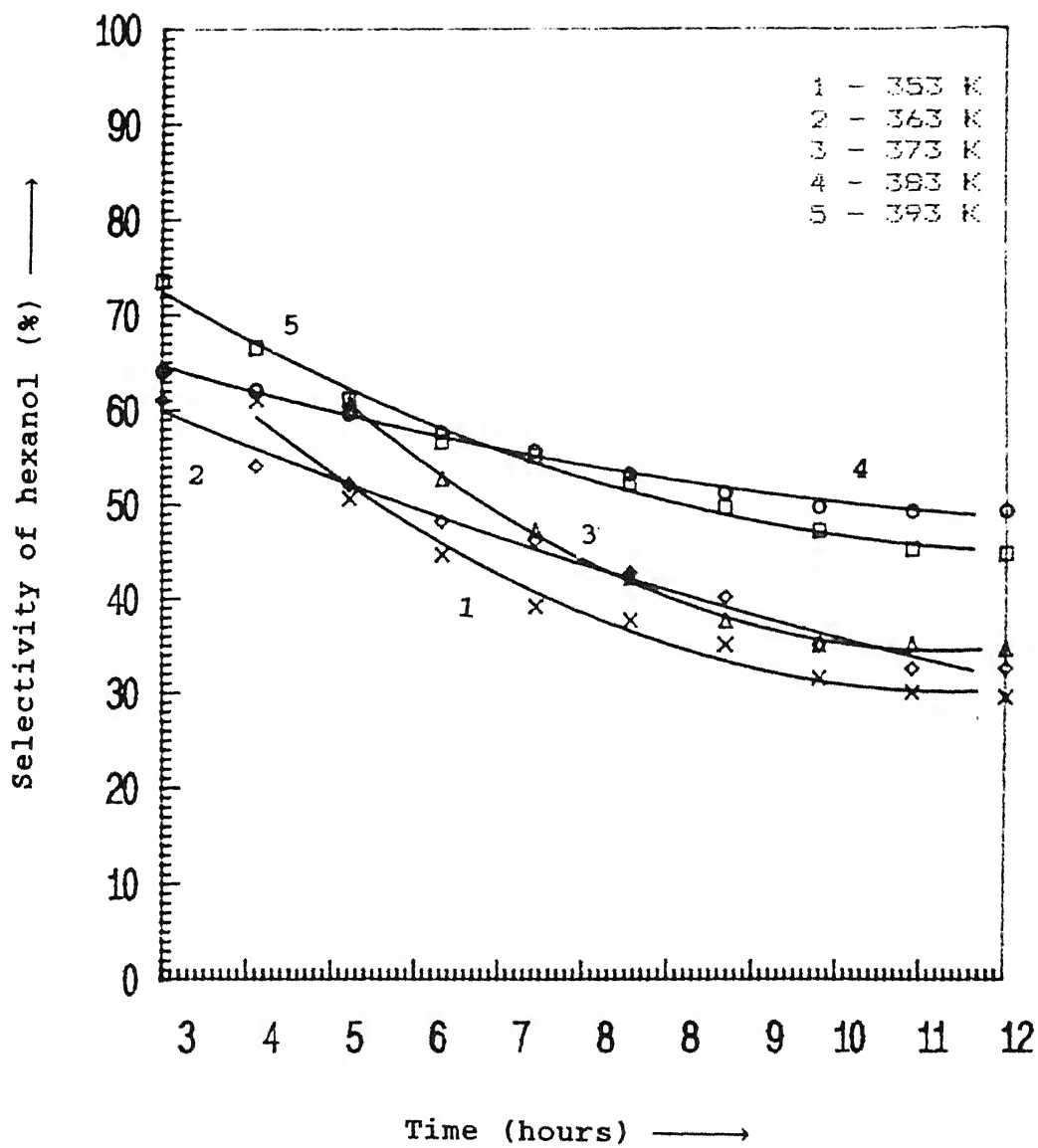


Fig 4.15 % Selectivity of Hexanol versus Time

(Temperature = 353 - 393 K, % Catalyst Loading = 1.5,
 $\text{H}_2\text{O}_2/\text{n-Hexane}$ Mole Ratio = 0.2)

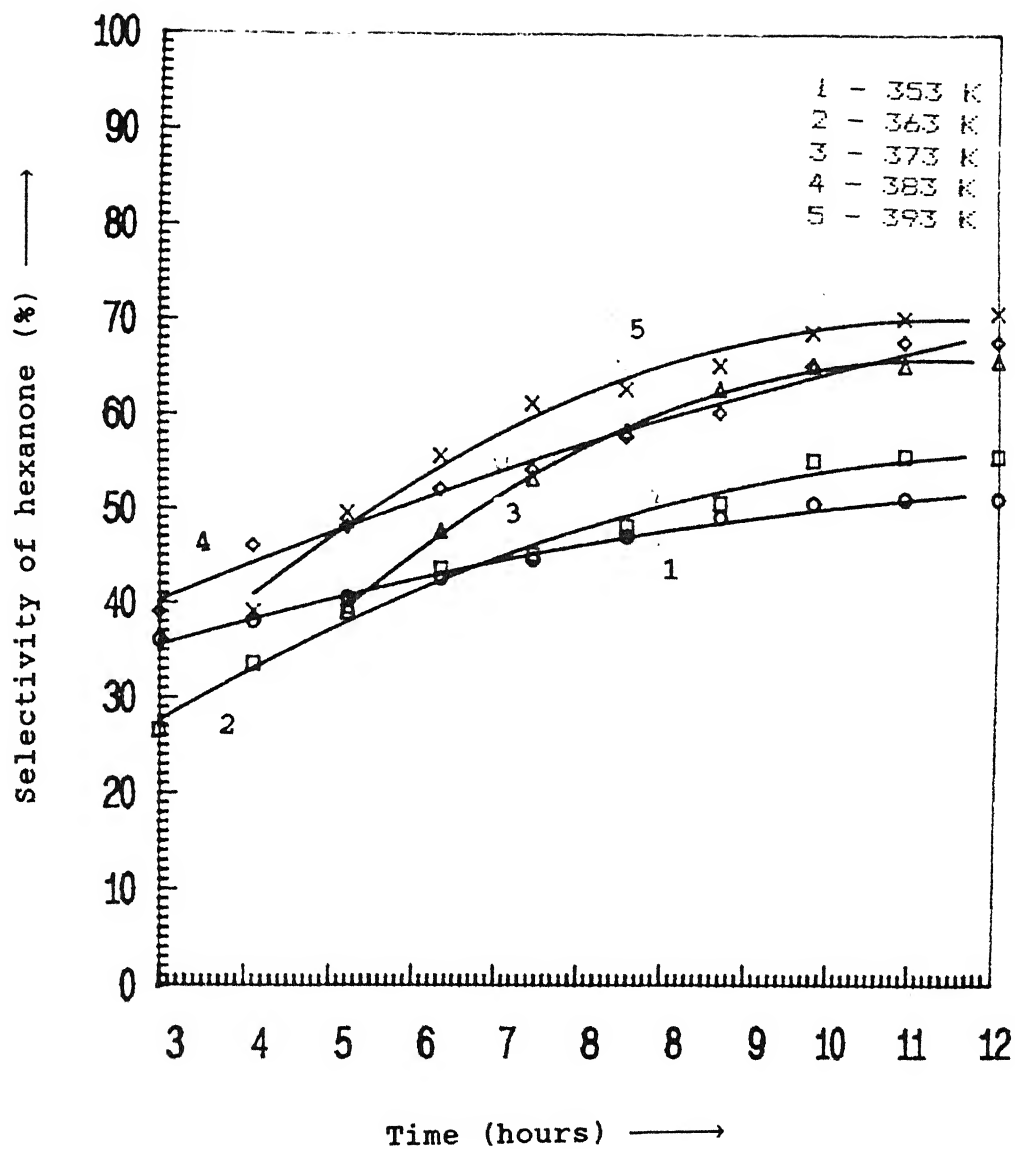


Fig 4.16 % Selectivity of Hexanone versus Time

(Temperature = 353 - 393 K, % Catalyst Loading = 1.5,
 $\text{H}_2\text{O}_2/\text{n-Hexane}$ Mole Ratio = 0.2)

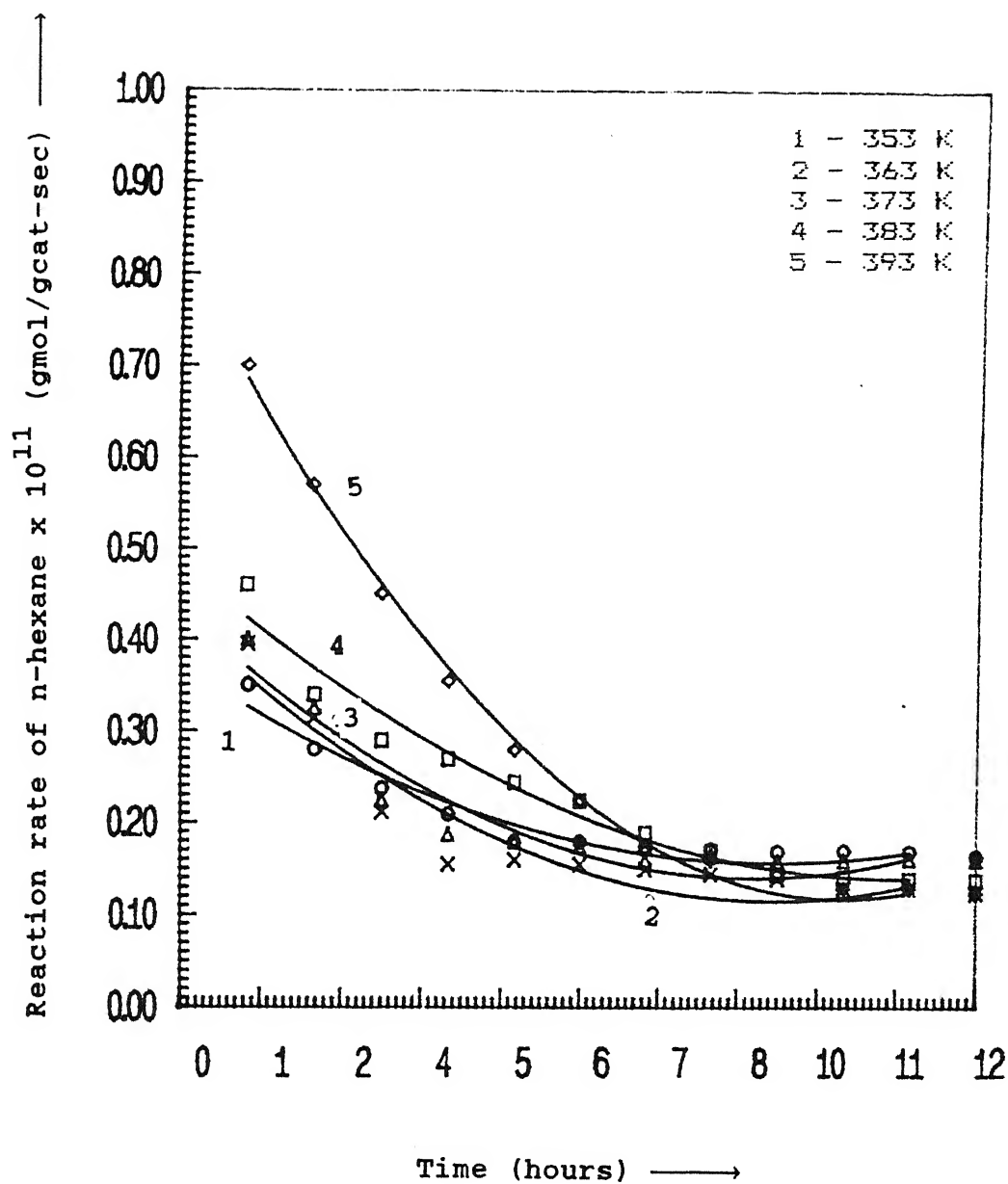


Fig 4.17 Rate versus Time (Temperature = 353 - 393 K,
 % Catalyst Loading = 1.5, H_2O_2 / n-Hexane Mole Ratio = 0.2)

Experimental rate, conversion, yield, selectivities of hexanol and hexanone were compared with that of calculated ones obtained from proposed kinetic models. Figures 4.18 to 4.21 show experimental values plotted against calculated values. It is clear from the figures that the experimental data were well correlated with calculated data. This further confirms that the proposed kinetic models predicted the data from the calculated reaction parameters well.

Table 4.15 shows the comparison of experimental and calculated values of conversion, yield and selectivities at different temperatures. Table 4.16 shows the comparison between the experimental values obtained and the reported values in the literature.

Table 4.15 Comparison of experimental and calculated values of % Conversion, % Yield, and % Selectivities at different temperatures.

| Temperature °K | % Conversion | | % Yield | | % Selectivity of hexanol | | % Selectivity of hexanone | |
|-------------------|--------------|-------|---------|-------|-----------------------------|-------|------------------------------|-------|
| | Expt. | Calc. | Expt. | Calc. | Expt. | Calc. | Expt. | Calc. |
| 353 | 25.8 | 27.5 | 43.0 | 40.1 | 59.0 | 55.0 | 41.0 | 45.0 |
| 363 | 25.5 | 26.8 | 47.0 | 48.1 | 40.0 | 38.0 | 60.0 | 62.0 |
| 373 | 34.8 | 33.3 | 54.0 | 52.6 | 39.0 | 41.3 | 61.0 | 58.0 |
| 383 | 40.9 | 41.4 | 61.0 | 58.1 | 54.0 | 50.0 | 46.0 | 50.0 |
| 393 | 54.3 | 58.4 | 62.0 | 60.0 | 44.0 | 42.0 | 56.0 | 58.0 |

Table 4.16 Comparision of Conversion, Yield and Selectivities with the Reported Values

| | Presented values | Reported Values |
|------------------------------------|------------------|-----------------|
| Conversion of <i>n</i> -hexane (%) | 58 | 44.5 |
| Yield of hexanol + hexanone (%) | 92.3 | 88.6 |
| Selectivity of hexanol (%) | 13 | 40.2 |
| Selectivity of hexanone (%) | 57 | 59.8 |

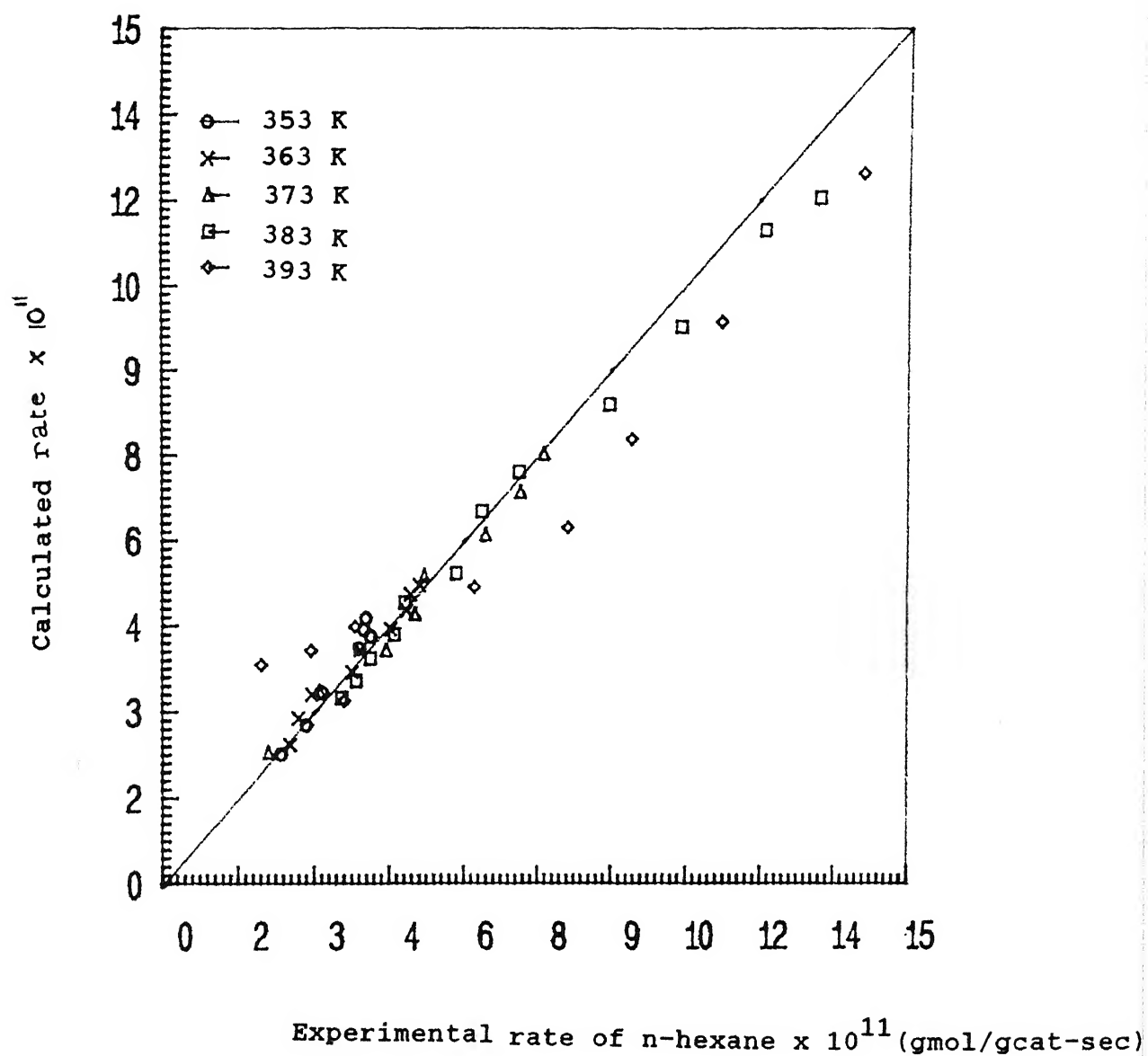


Fig 4.18 Comparison of Experimental versus Calculated Values of Rate of n-Hexane Over TS-1 Catalyst

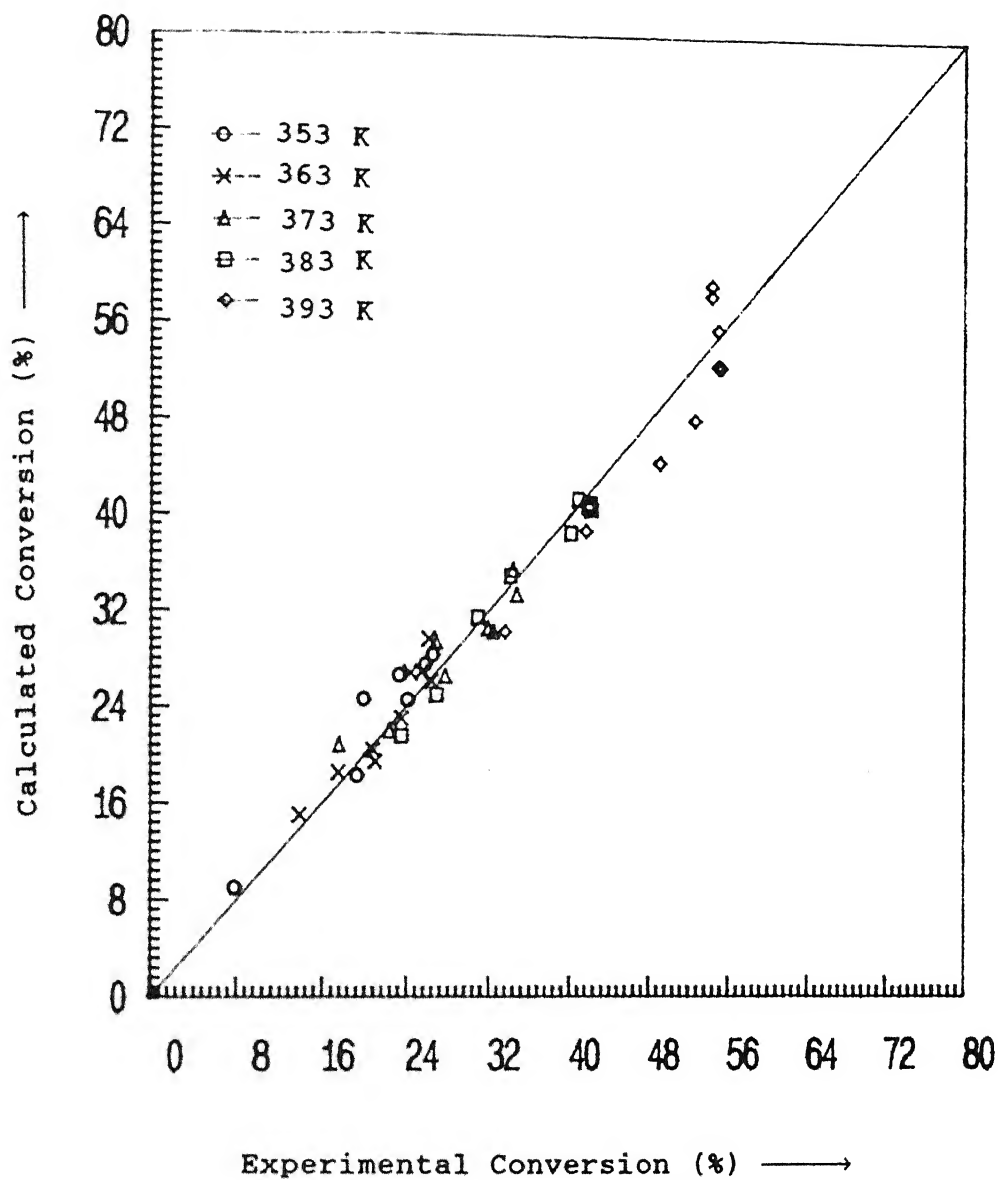


Fig 4.19 Comparison of Experimental versus Calculated Values of % Conversion of n-Hexane Over TS-1 Catalyst

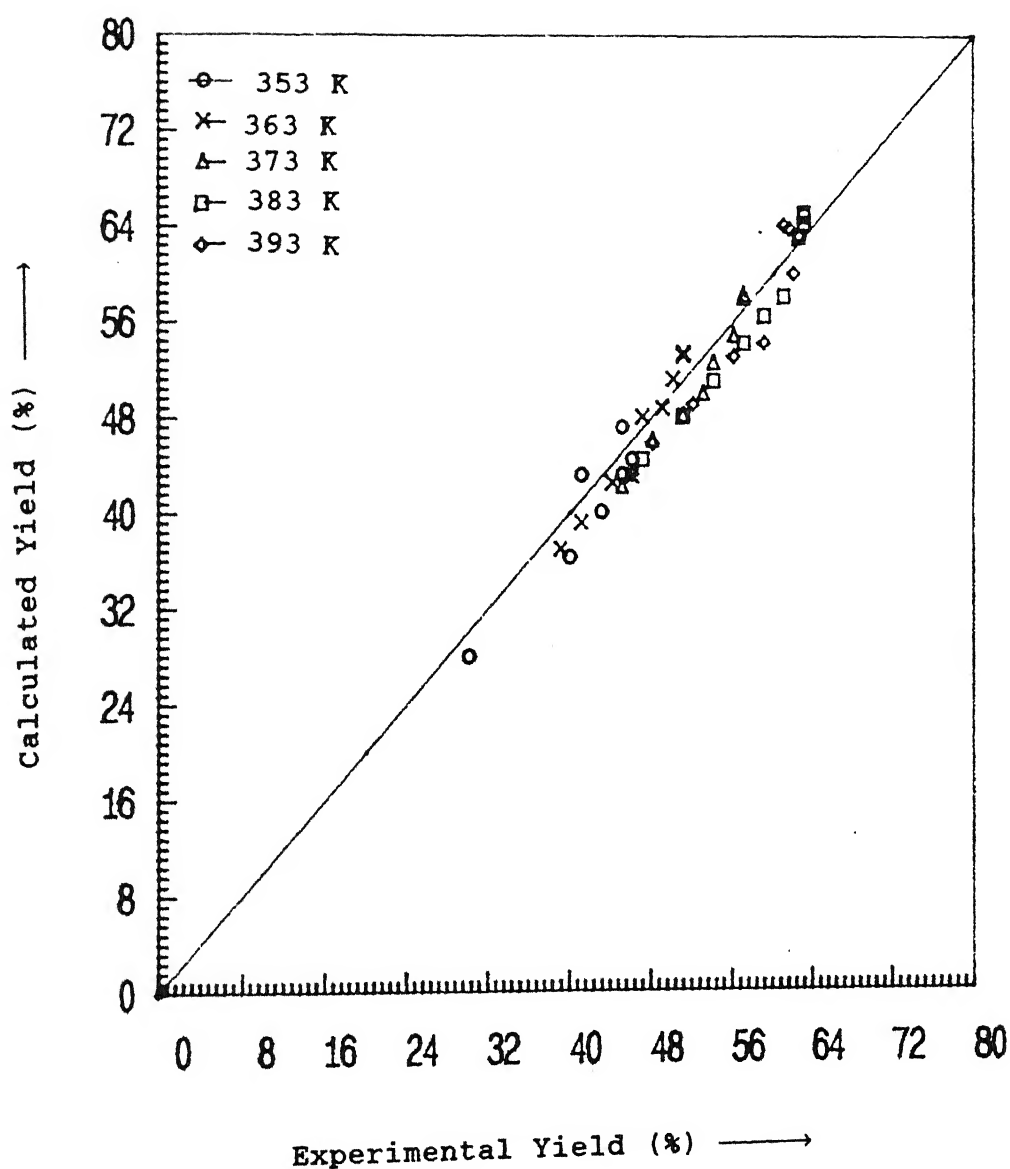


Fig 4.20 Comparison of Experimental versus Calculated Values of % Yield of Hexanol +Hexanone Over TS-1 Catalyst

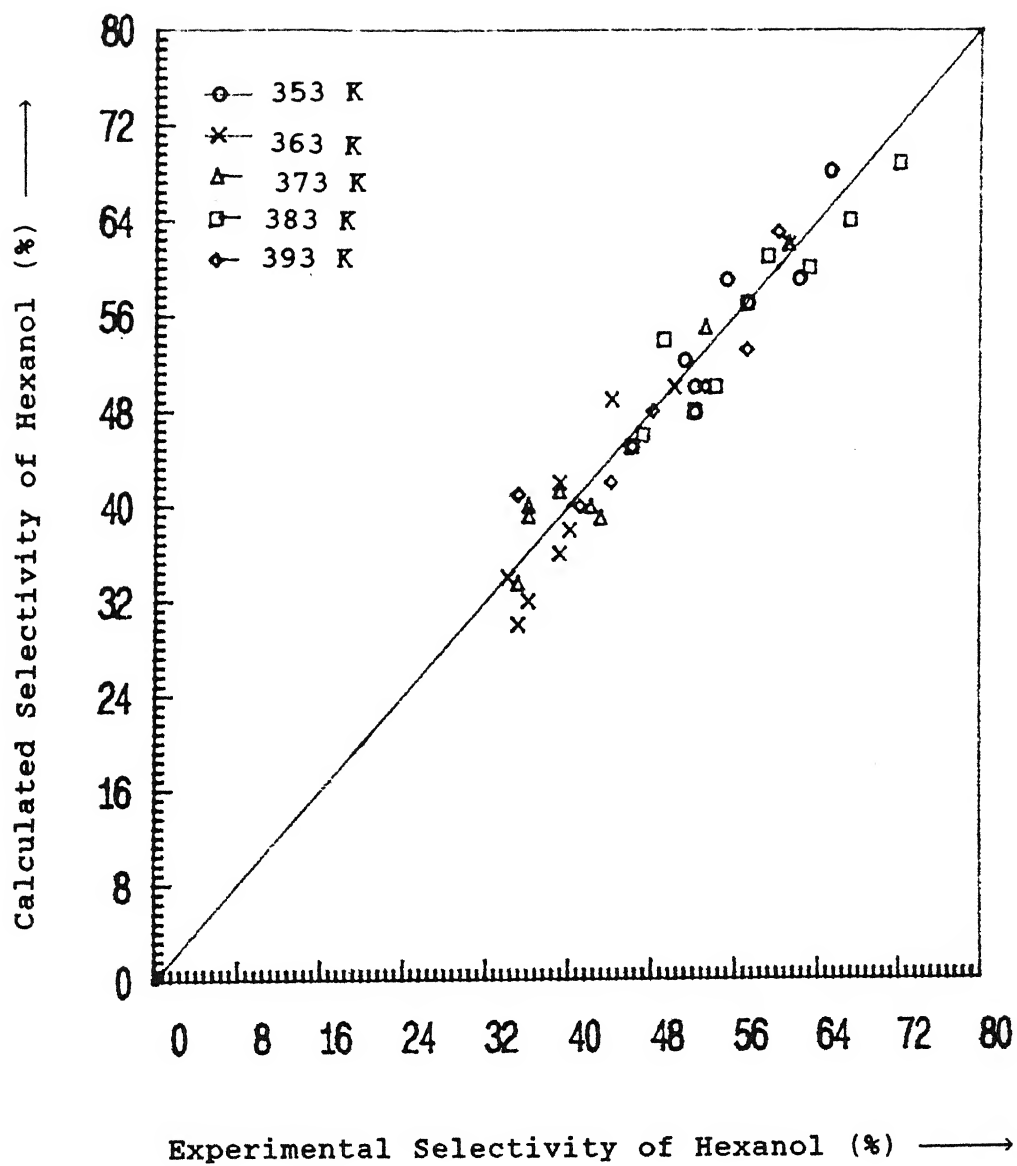


Fig 4.21 Comparison of Experimental versus Calculated Values of % Selectivity of Hexanol Over TS-1 Catalyst

CHAPTER 5

Conclusions and Recommendations

5.1 Conclusions

1. Kinetics of oxidation reaction between *n*-hexane and hydrogen peroxide was carried in a batch reactor over *TS* – 1 catalyst in liquid phase under autogeneous pressure using acetone as solvent.
2. Effect of important reaction variables such as reaction temperature (353–393 *K*), time (3–12 hrs), catalyst loading (1.5%–3.0%), H_2O_2/n -hexane mole ratio (0.2–1.4) and Ti content in *TS* – 1 catalyst ($Ti/(Ti+Si)=0.025 - 0.035$) were studied.
3. Conversion, yield and selectivities were found to be dependent on time, temperature, %catalyst loading, H_2O_2/n -hexane mole ratio and Ti content in *TS* – 1 catalyst. With increase in all above variables the conversion of *n*-hexane and yield of hexanol + hexanone were found to increase while the hexanol/hexanone ratio decreased.
4. XRD studies confirmed that a MFI structure (pentasil type) was obtained. IR studies revealed that Ti^{4+} ions were incorporated in MFI structure by isomorphous substitution. SEM studies revealed that the particle size of *TS* – 1 is very small with cuboid shape. With increase of Ti content the particle size was spherical with irregular surface.
5. Kinetic parameters were estimated from proposed rate models and experimental data were compared with calculated values obtained from rate models. There was a good agreement between the calculated and experimental values, thus confirming the validity of the models proposed.

6. Optimum values of reaction variables to get maximum yield of hexanol+hexanone were obtained by RSM.

$$H_2O_2/n\text{-hexane (mole ratio)} = 1.4$$

$$\text{Reaction time} = 8.48 \text{ Hrs.}$$

$$\text{Reaction temperature} = 377 \text{ K}$$

$$\% \text{ Catalyst loading} = 2.33$$

5.2 Recommendations

1. Higher value of Titanium content in *TS* – 1 catalyst gave good yields. Attempts should be made to introduce more titanium by isomorphous substitution technique. Other types of titanium silicalites such as *TS* – 2 with MEL structure should also be synthesized.

2. Crystallization of *TS* – 1 under stirring conditions will give smaller crystal size which may help in better yields. Results may be obtained on different crystal size to ascertain the effect of diffusion in the oxidation reaction.

3. TiZSM-5 catalyst prepared by CVD gave encouraging results, therefore, it should be further studied.

4. Oxidation studies of other alkanes and aromatics may be carried out over *TS* – 1 and *TS* – 2 catalyst. Attempts should be made to introduce other elements like Vanadium, by isomorphous substitution in MFI and MEL structure to get vanadium silicates which are promising catalysts for oxidation reactions.

REFERENCES

1. Behrens, P., Flesche, J., Vetler, S., Schulz Ekloff, G., Jaeger, N., Niemann, W., J. Chem. Soc. Chem. Commun., 1991, 678
2. Boccuti, M.R., Rao, K.M., Zecching, A., Leofani, T.G., and Petrini, G., in "Structure and Reactivity of Surfaces". (Morterra, C., et al., Eds.), studies in surface science and catalysis, Vol. 48, p. 133, Elsevier, Amsterdam, 1989.
3. Box, G.E.P., Youle, P.V. The exploration and explanation of Response. An example of link Between two Fitted surface and the Basic mechanism of the system. Biometrics 1953, 287-323.
4. Box, G.E.P., Hunter, W.G., Hunter, J.S. Statistics for Experimenters; John Wiley and Sons. New York, 1978, Chapter 10-12.
5. Box, G. E. P., Wilson, K. B. On The Experimental Attainment of Optimal Conditions. J. Roy. Statist. Soc. 1951, B 13, 1-45
6. Clark, R.J.H., "Chemistry of Titanium and Vanadium", p. 272, Elsevier, Amsterdam, 1967.
7. Clerici, M.G., Appl. Catal. 66 (1991) 249.
8. Cochran, W.G.; Cox, G.H. Exptl. Designs, 2nd ed.; John Wiley Inc. New York, 1957
9. Companion, A.L., and Wyatt, R.E., J. Phy. Chem. Solids, 24, 1025 (1963).
10. Davis, O.L. Design and Analysis of Independent Experiments, 2nd ed. Hafner Publ. Co. New York, 1956
11. Draper, N.R., Smith, M. Applied Regression Analysis, 2nd ed.; John Wiley and sons Inc. New York, 1981, 1-125.

12. Gilbert F.Froment, Kenneth B.Bischoff. Chemical Reactor Analysis and Design, 2nd ed, John Wiley and sons .Inc, NewYork, 1990, 61-124.
13. Gupta S.K., Numerical Calculations for Chemical Engineers, Wiley Eastern, 1988.
14. Hill.W.J, Hunter,W.G., A Review of Response Surface Method. A Literature Survey. Technometrics, 1966, 8, 571-590.
15. Huybrechts,D.R.C., DeBruycker,L and Jacobs ,P.A., Nature, 345 (1990) 240
16. Jacques Vedrigne,C., General Overview of Characterization of Zeolites; Zeolite Microporous Solids: Synthesis, Structure and Reactivity, 1992, 107 (13).
17. Krauschaar,B., and van Hoof,J.H.C., Catal.Lett.1 , 81 (1988).
18. Kuei -Jung Chao, Tseng Chang Tasi and Mei-Shu Chen, J.Chem.Soc.,Faraday Trans.1, 77 (1981), 547-555.
19. Kuester and Mize, Optimization techniques in Fortran., 1973, p.320.
20. Levenspiel,A.H, Chemical Reaction Engg. 2nd ed. W,Wiley Eastern Ltd, NewYork, 1985, 41-92.
21. Mamoru Ai., J.Catal. 54, 223 (1978)
22. Notari,B. Stud.Surf.Sci.Catal., 37 (1987) 413-423
23. Parton,R.F, Huybrechts,D.R.C, Buskens,*Ph*, Jacobs,P.A. Stud.Surf.Sci.Catal. 65 (1990) 47
24. Reddy,T.S., Kumar,*R*, and Ratnasamy,P. Appl.Catal., 58, L1 (1990)
25. Romano,U., Eposito,A., Maspero,F., Neri,C., and Clerici,M.G., Stud.Surf.Sci.Catal., 55 (1990) 33-41.
26. Taramasso,M., Perego,G., and Notari,B., US Pat. 4 410501 (1983).

27. Tatsumi,T., Nakanura,M., Nagishi,S., and Tominaga,H. J.Chem.Soc.Chem.Commun.
474. 1990
28. Thangaraj ,A., Kumar,R.,and Ratnasamy,P., Appl.Catal, 57, L1 (1991).
29. Thangaraj ,A., Kumar,R., and Ratnasamy,P., J.Catal , 131, 294 (1991).
30. vander Pol,A.J.H.P., and van Hoof, J.H.C., Appl.Catal, 92 (1992) 93-111.

Appendix A

Kinetic Data for $TS - 1$ catalyst. H_2O_2/n -hexane mole ratio = 0.2

% Catalyst loading (gm catalyst/ gmm -hexane $\times 100$) = 1.5

Reaction Temperature = 353K

| Time hours | C_A gmol/cc 10^{+3} | C_B gmol/cc $\times 10^{+3}$ | C_C gmol/cc $\times 10^{+3}$ | C_D gmol/cc $\times 10^{+3}$ | Rate gmol/gcat-sec $\times 10^{+11}$ |
|---------------|-------------------------------|--------------------------------------|--------------------------------------|--------------------------------------|--|
| 3 | 6.118 | 4.63 | 1.25 | 0.82 | 4.32 |
| 6 | 5.43 | 3.85 | 0.989 | 1.445 | 4.64 |
| 7 | 4.78 | 3.62 | 0.965 | 1.648 | 4.44 |
| 8 | 4.63 | 3.47 | 0.953 | 1.783 | 4.11 |
| 10 | 4.2 | 3.41 | 0.63 | 1.365 | 3.33 |
| 11 | 4.15 | 3.4 | 0.45 | 1.318 | 2.77 |
| 12 | 4.12 | 3.41 | 0.35 | 1.4 | 2.27 |

Reaction Temperature = 363K

| Time hours | C_A gmol/cc 10^{+3} | C_B gmol/cc $\times 10^{+3}$ | C_C gmol/cc $\times 10^{+3}$ | C_D gmol/cc $\times 10^{+3}$ | Rate gmol/gcat-sec $\times 10^{+11}$ |
|---------------|-------------------------------|--------------------------------------|--------------------------------------|--------------------------------------|--|
| 4 | 5.57 | 4.24 | 1.55 | 0.99 | 5.22 |
| 5 | 5.38 | 4.00 | 1.32 | 1.38 | 5.05 |
| 6 | 5.10 | 3.79 | 1.82 | 1.13 | 4.77 |
| 7 | 4.96 | 3.61 | 1.20 | 1.84 | 4.44 |
| 8 | 4.20 | 3.48 | 0.80 | 1.89 | 4.08 |
| 9 | 3.99 | 3.42 | 0.20 | 2.00 | 3.69 |
| 10 | 3.80 | 3.40 | 0.45 | 1.61 | 3.30 |
| 11 | 3.75 | 3.25 | 0.30 | 1.40 | 2.89 |
| 12 | 3.70 | 3.20 | 0.25 | 1.10 | 2.43 |

Reaction Temperature = 373K

| Time hours | C_A gmol/cc $\times 10^{+3}$ | C_B gmol/cc $\times 10^{+3}$ | C_C gmol/cc $\times 10^{+3}$ | C_D gmol/cc $\times 10^{+3}$ | Rate gmol/gcat-sec $\times 10^{+11}$ |
|---------------|--------------------------------------|--------------------------------------|--------------------------------------|--------------------------------------|--|
| 4 | 5.88 | 3.68 | 1.98 | 0.90 | 7.53 |
| 5 | 5.46 | 3.34 | 1.26 | 1.34 | 6.86 |
| 6 | 4.67 | 3.06 | 1.17 | 2.26 | 6.11 |
| 7 | 4.20 | 2.90 | 0.93 | 2.30 | 5.39 |
| 8 | 4.20 | 2.88 | 0.80 | 2.58 | 4.72 |
| 9 | 3.78 | 2.74 | 0.75 | 2.61 | 4.08 |
| 10 | 2.73 | 2.75 | 0.70 | 2.95 | 3.36 |
| 11 | 2.75 | 2.65 | 0.75 | 1.75 | 2.30 |
| 12 | 2.75 | 2.60 | 0.70 | 1.20 | 1.95 |

Reaction Temperature = 383K

| Time hours | C_A gmol/cc $\times 10^{+3}$ | C_B gmol/cc $\times 10^{+3}$ | C_C gmol/cc $\times 10^{+3}$ | C_D gmol/cc $\times 10^{+3}$ | Rate gmol/gcat-sec $\times 10^{+11}$ |
|---------------|--------------------------------------|--------------------------------------|--------------------------------------|--------------------------------------|--|
| 3 | 4.98 | 3.61 | 1.53 | 1.53 | 9.77 |
| 4 | 4.76 | 3.39 | 1.75 | 1.75 | 8.40 |
| 5 | 4.50 | 3.13 | 2.01 | 2.01 | 7.22 |
| 6 | 4.28 | 2.92 | 2.22 | 2.23 | 6.53 |
| 7 | 3.90 | 2.53 | 2.61 | 2.61 | 5.44 |
| 8 | 3.85 | 2.48 | 2.66 | 2.66 | 4.92 |
| 9 | 3.78 | 2.42 | 2.72 | 2.72 | 4.36 |
| 10 | 3.77 | 2.41 | 2.73 | 2.73 | 3.94 |
| 11 | 3.77 | 2.40 | 2.73 | 2.74 | 3.55 |
| 12 | 3.76 | 2.39 | 2.71 | 2.75 | 3.25 |

Reaction Temperature = 393K

| Time hours | C_A gmol/cc 10^{+3} | C_B gmol/cc $\times 10^{+3}$ | C_C gmol/cc $\times 10^{+3}$ | C_D gmol/cc $\times 10^{+3}$ | Rate gmol/gcat-sec $\times 10^{+11}$ |
|---------------|-------------------------------|--------------------------------------|--------------------------------------|--------------------------------------|--|
| 3 | 5.63 | 2.95 | 2.16 | 1.41 | 12.47 |
| 4 | 5.04 | 2.42 | 1.49 | 1.45 | 9.86 |
| 5 | 4.83 | 2.01 | 1.47 | 2.10 | 7.80 |
| 6 | 4.20 | 1.72 | 0.97 | 2.60 | 6.25 |
| 7 | 4.07 | 1.54 | 0.84 | 2.81 | 5.20 |
| 8 | 3.36 | 1.50 | 0.55 | 2.98 | 4.50 |
| 9 | 2.93 | 1.15 | 0.50 | 2.62 | 4.08 |
| 11 | 2.95 | 1.40 | 0.45 | 2.20 | 3.83 |
| 12 | 2.85 | 1.41 | 0.40 | 2.10 | 3.20 |